CHARACTERIZATION OF THE LINKAGE BETWEEN XYLOGLUCAN AND PECTIN IN ARABIDOPSIS THALIANA CULTURE CELL WALLS

By

XIAOYU QIAO

Bachelor of Science in Biological Sciences
Jilin University
Changchun, Jilin Province, China
2009

Master of Science in Biochemistry and Molecular Biology
Jilin University
Changchun, Jilin Province, China
2012

Submitted to the Faculty of the
Graduate College of the
Oklahoma State University
in partial fulfillment of
the requirements for
the Degree of
DOCTOR OF PHILOSOPHY
July, 2021

CHARACTERIZATION OF THE LINKAGE

BETWEEN XYLOGLUCAN AND PECTIN IN

ARABIDOPSIS THALIANA CULTURE CELL WALLS

Dissertation Approved:

Dr Andrew Mort

Dissertation Adviser

Dr Robert Matts

Dr Junpeng Deng

Dr Rolf Prade

.

ACKNOWLEDGEMENTS

It is a great privilege to study with my advisor Dr. Andrew Mort, who has been patient, inspiring and enthusiastic. Dr Mort helped me to interpret research and overcome setbacks with his scientific experience, dialectical thinking, and kind encouragements.

I would also like to express my appreciation to my committee members Dr. Robert Matts, Dr. Junpeng Deng, Dr Rolf Prade for their precious advice with my thesis; to Dr Steve Hartson and Janet Rogers for their valuable suggestions with mass spectrometry; and to Dr. Margaret Eastman and Dr. Xiangmei Wu for their insightful guidance with NMR experiments. I am also grateful to Dr. Guru Jagadeeswaran, Dr Lawrie Gainey and department of biochemistry and molecular biology for their kind support, and to Department of Energy for their generous funding.

Finally yet importantly, I would like to thank my parents and my sister for their unconditional love. I missed years of time with my family, and I felt especially sorry for not being there for them during the pandemic, yet they still encourage me to pursue my academic goal with great understanding and wholehearted support.

Name: XIAOYU QIAO

Date of Degree: July, 2021

Title of Study: CHARACTERIZATION OF THE LINKAGE BETWEEN XYLOGLUCAN AND PECTIN IN ARABIDOPSIS THALIANA CULTURE CELL WALLS

Major Field: BIOCHEMISTRY AND MOLECULAR BIOLOGY

Abstract: Xyloglucan, a major cross-linking glycan in the primary cell wall of most eudicots, has been considered to be independent of the pectic network. However, several groups have found strong evidence for a covalent attachment to pectin in walls of cell cultures. There has only been speculation on the nature of the linkage between xyloglucan and pectin. Isolation of a crosslinking fragment between pectin and xyloglucan has been elusive. The Mort lab has been working on this for thirty years with limited success. We isolated the pectin-associated xyloglucan from *Arabidopsis thaliana* suspension cell cultures using anion exchange chromatography. Endo-arabinanase was then used to release xyloglucan from the pectin. An arabinose residue was found in dissociated xyloglucan and found to be at the reducing end instead of sidechains of the released xyloglucan. A similar arabinose-containing linkage was also found in the pectin-unbound free xyloglucan, possibly existing as an intermediate of xyloglucan-pectin conjugation. Part of the pectin-associated xyloglucan was not covalently linked to the pectin. Such a tight non-covalent interaction survived strong alkali, heat, and concentrated salt elution. Debranching rhamnogalacturonan-I with exo-arabinosidase or heating at 80℃ could release much of the non-covalently bound xyloglucan. Much remains to be learned about the interactions between pectins and xyloglucans and their roles in cell wall function.

TABLE OF CONTENTS

LIST OF TABLES

Table Page

LIST OF FIGURES

Figure Page

ABBREVIATIONS

Glc	glucose
Xyl	xylose
Gal	galactose
Fuc	fucose
Ara	arabinose
Rha	rhamnose
GalA	galacturonic acid
Hex	hexose
Pen	pentose
p	pyranose
f	furanose
t	terminal
i	internal
r.e.	reducing end
perMe	permethylated
TMS	trimethylsilyl
DMSO	dimethyl sulfoxide
FA	formic acid
HAc	acetic acid
NH_4Ac	ammonium acetate

XG or XyGs	xyloglucans
GAX	glucuronoarabinoxylan
HG	homogalacturonan
XGA	xylogalacturonan
RG II	rhamnogalacturonan II
RG I	rhamnogalacturonan I
AGs	arabinogalactans
AGPs	arabinogalactan proteins
HRGPs	hydroxyproline-rich glycoproteins
PRPs	proline-rich proteins
GRPs	glycine-rich proteins
XEG	xyloglucan-specific endo-glucanase, or xyloglucanase
PGase	polygalacturonase
EPG	endo polygalacturonase
PME	pectin methylesterase
CZE	capillary zone electrophoresis
ANTS	8-aminonaphthalene-1,3,6-trisulfonic acid
APTS	8-aminopyrene-1,3,6-trisulfonic acid
2-AB	2-aminobenzamide
5AN1S	5-aminonaphthalene-1-sulfonic acid
5AN2S	5-aminonaphthalene-2-sulfonic acid
GC	gas chromatography
LC	liquid chromatography
AEC	anion exchange chromatography
HILIC	hydrophilic interaction chromatography

RPC	reversed-phase chromatography
PGC	porous graphitic carbon column
MS	mass spectrometry
MALDI-TOF	matrix-assisted laser desorption/ionization-time of flight
DHB	2,5-dihydrozybenzoic acid
ESI-LC-MS/MS	electro-spray ionization-liquid chromatography-tandem mass spectrometry
NMR	nuclear magnetic resonance spectroscopy
TOCSY	total correlation spectroscopy
HSQC	heteronuclear single quantum coherence
HMBC	heteronuclear multiple bond correlation
NOESY	nuclear overhauser effect spectroscopy

CHAPTER I

INTRODUCTION

Plant cell wall

The plant cell wall is a dynamic compartment wrapping around the outside of the plant cell membrane. As a plant cell grows and divides, new material is synthesized, transported and woven into a thin layer of primary cell wall to maintain the size and shape of the plant cell. Middle lamella forms during cell division, grows coordinately with primary walls and promotes adherence between walls of two adjacent cells. Secondary wall is deposited between the primary wall and the plasma membrane after cell growth ceases providing mechanical stability to the plant. (Carpita 2015). Besides its structural attributes, the plant cell wall extensively affects cell growth, development and differentiation by participating in intra- and inter-cellular communication, cell positioning, determining growing polarity, stimuli response and defense, etc.

Composition

Wall composition and molecular structure can vary among species, different tissues of the plant, and different stages of growth. Dicot primary plant cell wall is mainly comprised of

celluloses, hemicelluloses, pectic polysaccharides, and structural proteins. Hemicelluloses and pectins, together called matrix polysaccharides, are assembled in the Golgi apparatus, and transferred to the apoplast by vesicles. Cellulose microfibrils, the load-bearing scaffold, are synthesized at the plasma membrane and tethered by hemicelluloses; this framework is embedded in a gel of pectic polysaccharides.

Cellulose is composed of linear β- (1→4) - D-glucans thousands of residues long (Figure 1.1.A). In vascular plants, dozens of glucan chains align parallel to each other by hydrogen bonding and form a para-crystalline microfibril nanometers wide with reducing ends pointing in the same direction (Figure 1.1.B); the microfibril can be hundreds of micrometers long as multiple individual glucan chains converge along the length at different places within the microfibril. The bundle-style arrangement greatly enhances the rigidity of microfibrils by restraining the conformation of glucan chains, while glucan polymers on the surface of cellulose microfibrils can associate with other glycans or water.

A

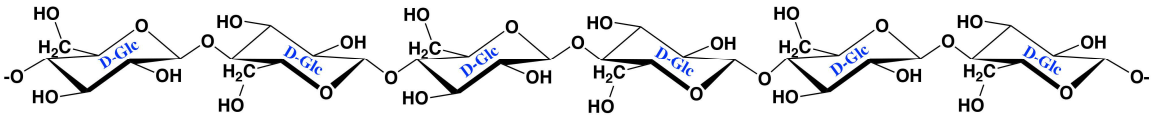

B

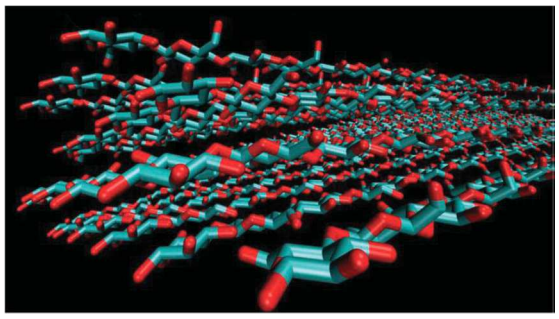

Figure 1.1 A. β- (1→4) - D-glucan. Residues are almost 180° inverted from each other to produce a nearly linear chain. B. Molecular modeling of a cellulose microfibril. (Mike Crowley, National Renewable Energy Lab, Golden, CO.)

Hemicellulose are a class of crosslinking polysaccharides extracted from the cell wall with strong alkali. Those crosslinking glycans can interlock the cellulose scaffold by coating or anchoring cellulose microfibrils through hydrogen bonding to form a network.

Xyloglucans (XGs or XyGs) are the major crosslinking glycans in primary cell walls of most eudicots and half of the monocots. Typical XG consists of linear β- (1→4) - D-glucan as backbone, with three adjacent residues out of every four Glc residues being substituted at O-6 position with α-D Xyl residues leaving one Glc residue unbranched. Naked xyloglucans are poorly soluble, some xylosyl units are further substituted at O-2, for instance in *Arabidopsis*, commonly with β-D Gal-(1→, or α-L-Fuc-(1→2)-β-D-Gal-(1→, those sidechains initiated from Glc are designated with a single-letter code, L and F respectively, on the basis of their terminal sugar. Correspondingly, X denotes Glc solely substituted with Xyl, while G denotes the unsubstituted backbone Glc residue. (Figure 1.2)

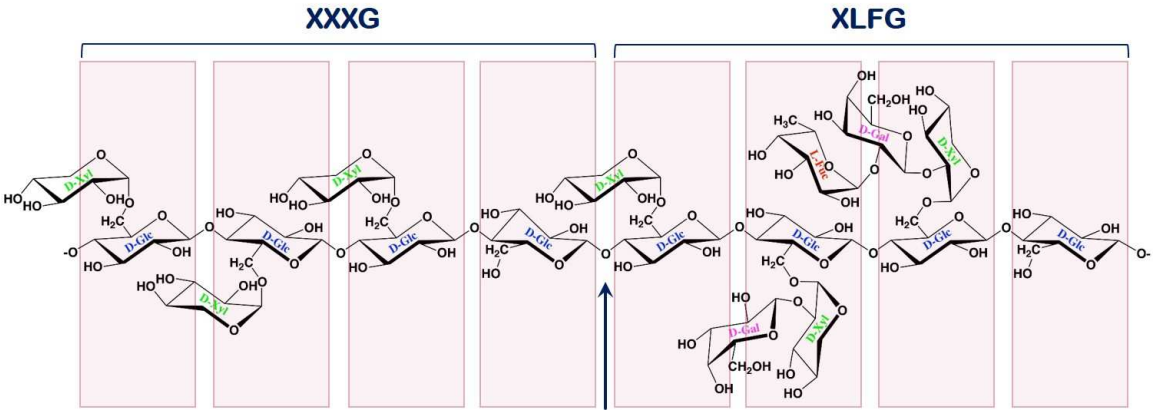

Figure 1.2 A xyloglucan segment comprising of two common subunits XXXG and XLFG. Arrows indicate the hydrolysis site of xyloglucan-specific endo-glucanase.

The composition and distribution of xyloglucan side-chains vary among species; these branches are considered to improve aqueous solubility, segregation amid scaffold glycans, and to affect the substrate specificity of wall-modifying enzymes. The unsubstituted backbone Glc

residues are recognized and cleaved by xyloglucan-specific endo-glucanase (XEG), giving rise to signature subunits with the unbranched Glc residues at reducing ends (Figure 1.2). In Arabidopsis, the predominant subunits are XXXG, XXLG, XLXG, XXFG and XLFG. Ratios and compositions of these XG-constructing blocks are often characteristic in different plants. XEG digestion products can be analyzed with capillary electrophoresis to indicate the presence of xyloglucan. Xyloglucan is also found to be O-acetylated, usually on O-2 or O-3 of galactose (Kiefer 1989). However, such ester linkages are usually cleaved by the strong alkali, which is typically used to extract hemicelluloses from cell walls.

There are also other minor crosslinking glycans, such as glucuronoarabinoxylans (GAX), mixed-linked (1→3),(1→4)-β-D-glucans (β-glucans), mannans, glucomannans and galactoglucomannans, which vary in composition and in size among different plant species. These glycans are much less abundant in primary walls of dicots, but some might be alternatives to xyloglucan and function as major crosslinking polymers, like GAX in commelinid monocots and β-glucans in Poales; some even replace the cellulose scaffold, such as mannan microfibrils in certain algae.

Pectin matrix polymers are galacturonic acid - rich polysaccharides, much of which can be extracted from cell walls with calcium chelators or de-esterifying agents such as alkali (<0.1M). Pectins are comprised of several domains, most of which have an α- (1→4)- D-galacturonan (homogalacturonan, HG) backbone (Figure 1.3 A). The HG domains contain up to 200 GalA residues and are about 100 nm long. The carboxyl groups of the GalA residues are often methyl esterified. Xylogalacturonan (XGA) domains are HG substituted with α-D-Xyl*p* at the O-3 position of around half of the GalA units (Figure 1.3 B). Low-abundance rhamnogalacturonan II (RG II) domains have an HG backbone substituted with diverse sugars; the structure is complicated yet highly conserved among flowering plants. RG-II can be

A

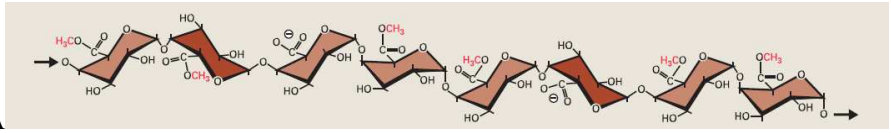

B

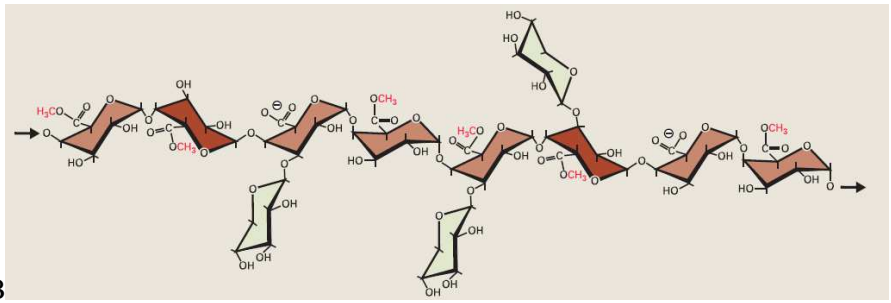

C

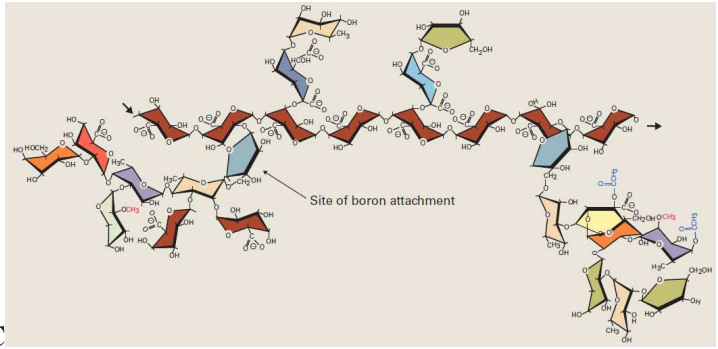

D

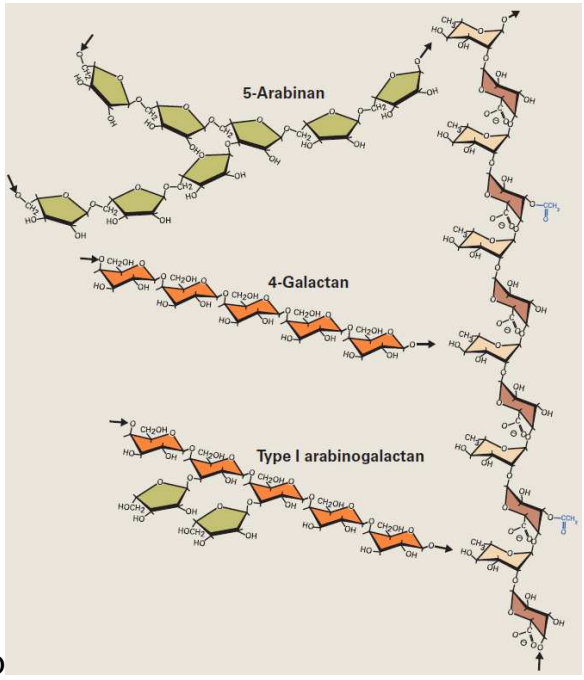

Figure 1.3 Pectin domains. A. Methyl esterified HG. B. XGA. C. RG-II. D. RG-I. (Carpita 2015)

dimerized by forming two di-ester bonds with borate at the apiose residues in the sidechains (Figure 1.3 C). Rhamnogalacturonan I (RG I) has a backbone of repeating (1→2)-α-L- Rha-(1→4)-α-D-GalA disaccharide units, different from the other pectic domains. Secondary hydroxyl groups of GalA units are often acetylated. Many Rha residues of RG-I are branched at the O-4 position with neutral sugar chains of diverse lengths and configurations, such as branched and linear α- (1→5)- L- arabinans, β - (1→4)- D- galactans, and type I arabinogalactans (AGs) which are β- (1→4)- D- galactan chains with mostly t- Ara at the O-3 of the Gal (Figure 1.3 D). Some of the RG-I can be extracted by polygalacturonase (PGase). The different pectic domains could be continuous with each other in one molecule, or cross-link noncovalently to form an intermolecular network. Branched pectins are highly hydrated and charged, and play important roles in inter-cellular adhesion, adjusting wall porosity, molecular signal transduction and responses to stresses.

Proteins in plant cell walls are mostly structural components (Cassab 1998), while others such as proteases and glycosyl hydrolases, play important roles in cell wall remodeling and turnover (Darley 2001). Wall structural proteins are named for their compositions: hydroxyproline-rich glycoproteins (HRGPs), proline-rich proteins (PRPs), and glycine-rich proteins (GRPs). They vary among tissues and species and adapt during different growth or development stages. Extensin, a plant secretory HRGP, is comprised of repeating Ser-$(Hyp)_4$ and Tyr-Lys-Tyr sequences with the Ser residues decorated with single t-α-D-Gal and the Hyp residues decorated with oligo-arabinans. Arabinogalactan proteins (AGPs) are a broad class of secretory proteins enriched in Pro (Hyp), Ala, and Ser/Thr. AGPs, more accurately proteoglycans, are heavily glycosylated with large type II arabinogalactans (AGs). Type II AGs are short branched β- D- galactan chains with (1→3)- and (1→6)- mixed glycosidic linkages in both backbones and branch points. The galactans are decorated with Ara residues, while t-β-D-GlcA-(1→3)- and t- α- L- Rha- (1→4)- β- D- GlcA- (1→3)- side groups are attached to the

(1→6)- β-D-galactan chains. Some AGPs with the C terminus cleaved enzymatically are covalently attached to glycosylphosphatidyl inositides (GPI) anchors during synthesis and secretion in the ER and Golgi apparatus. The glycolipids anchor the AGPs to the plasma membrane. The protein portion can be released by phospholipases, and then migrate either into the cell wall or back to the cytoplasm.

Architecture

Cell wall components and structures vary from algae to land plants having evolved to adapt to their environment. Primary cell wall architectures vary among species, tissues, and development stages. In a generic cell wall architecture model (Carpita 2015, McCann 2008, Vincken 2003), the celluloses are cross-linked by hemicelluloses, this framework is then embedded in another network of pectic matrix (figure 1.4), proteins and aromatic molecules assist the assembly as a third network, these networks in primary cell walls are considered to be functionally independent but structurally interacting with each other.

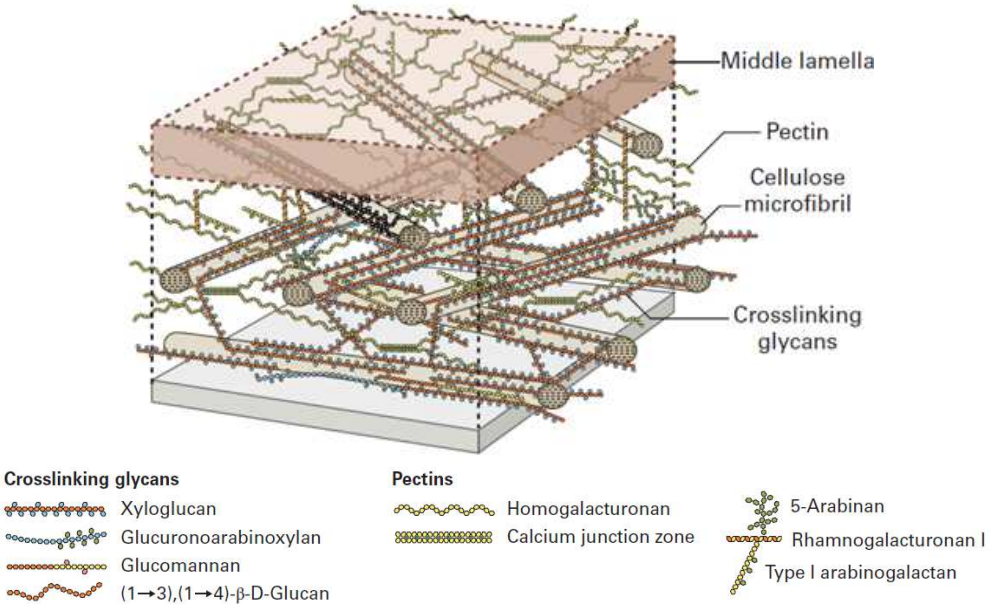

Figure 1.4 Molecular model of cell wall (Carpita 2015)**.**

Cellulose-crosslinking glycan network

Most eudicots walls contain similar amounts of cellulose and xyloglucan. Xyloglucans, the major crosslinking hemicelluloses, anchor to the surface glucans of different cellulose microfibrils with same backbone components, and span the distance between microfibrils to prevent adjacent microfibrils from aligning together too tightly. Xyloglucan-tethered cellulose microfibrils could still shift slightly when xyloglucans bend or swing by rotating the backbone glycosidic bonds (figure 1.4), which greatly benefit the elasticity and shaping of the cellulose-xyloglucan network. Such cellulose-spanning xyloglucans may also associate with other xyloglucans and glycans, while some other xyloglucans are free dispersed in primary wall with greater mobility and better access for enzymes. During growth or stimuli response, cellulose-xyloglucan network could be loosened and rearranged by enzymatically cleaving or peeling xyloglucans and interlacing more materials.

Pectin network

HG is usually highly methylesterified, however the negative charges of the carboxylate groups can be exposed by saponification or pectin methylesterase (PME), and then bind to cations such as calcium ions. Intermolecular calcium bridging may happen between antiparallel aligned HG chains converting soluble molecules into a gel. The more unesterified GalA units there are, the stronger the ion bridging crosslinks, if calcium ions are sufficient, some methyl esters can be tolerated at a junction, however the presence of methyl esters makes junction zone less firmly bound, loosens the gel network, and affects the charge density, local pH and matrix hydration. Ionic interaction brings GalA groups that are residues apart or on different molecules into close proximity, the spacing favors the porosity of pectin matrix. The Rha residues in RG-I and the sidechains prevent the GalA residues in RG-I from forming calcium bridges. This affects the

relative pore size of the walls. Molecules on the order of 10 kD or less diffuse freely through cell walls thanks to their porosity, which is determined by the frequency and length of ion-bridge junction, the degree of methyl esterification, the length and distribution of RG-I neutral side chains such as arabinans, galactans and arabinogalactans, and the frequency of RG-II regions which dimerize in the presence of boron. To adapt to growth and environmental stress, wall porosity can be modulated, for instance, by pectin methylesterase releasing more carboxylic groups, by adjusting the ion concentrations such as borate and calcium, or by enzymatically alternating the length of RG-I sidechains that are highly mobile within pore cavities.

Other networks

Proteins and aromatics also play important roles in cell wall construction. Structural proteins such as cortical microtubules guide the initial orientation of cellulose microfibrils synthesis. Others like extensins may participate the reinforcement of the cellulose-xyloglucan network during wall expansion by tethering separated microfibrils and complexing with other proteins. Expansins detach microfibrils and crosslinking glycans. Arabinogalactan proteins (AGPs) accumulate in Golgi apparatus and secretory vesicles, which possibly are to secure the wall material transportation and to temporarily anchor the intermediate composites. Glycosylation is crucial for maintaining the shapes of those proteins, may also contribute in the interactions with other wall components. Some proteins can covalently bridge with each other or with other glycans by glycosidic, peptide or ester bonds, and by ether or aryl linkages when involving aromatics like polyphenols in grass.

Integration of networks

During plant cell growth and mitosis, cell walls dynamically expand and extensively reconstruct by interlacing with newly synthesized polymers or salvaged intermediates. In specific tissues like root hairs and pollen tubes, expansion is focused at the apex of the cell so that the

elongation orients towards the tip. The cellulose-hemicellulose framework is loosened by hydrolases cleaving the tethering molecules or by expansins disassociating the crosslinking glycans. Growth of the wall is promoted by the turgor pressure of the protoplast. With the aid of transglycosylases, more newly synthesized microfibrils underpin and fuse with the inner face of existing wall to maintain the thickness and rigidity of growing wall. With the assistance of crosslinking glycans such as xyloglucans and structural proteins, microfibrils are deposited and woven in favored patterns, for example, in elongation, new microfibrils are considered to orient in helix-like trend around the axis so that the cells extend easily lengthwise rather than radially. When growth stops, microfibrils are tethered and secured again by crosslinking glycans, proteins or phenylpropanoids to stand against the turgor pressure.

The pectin network, the enclosing matrix, accommodates during the wall frame renovation. The network is loosened by enzymes as glycosyl transferases, hydrolases and lyases, the composition and distribution of the pectic polymers are engineered to fulfill the growing structure. Not only is covalent assembly altered, but noncovalent interactions, including hydrogen bonding, ionic bridging, and van der Waals' interaction, are also extensively involved during this process to maintain the integration and permeability. Pectic porosity, local pH, solubility and charge density greatly affect the migration and function of wall-modifying enzymes. Some wall components are secreted soluble with esterification or glycosylation, the esters or ethers are cleaved by modifying enzymes to expose crosslinking sites, then transferred to rearrange spacial distribution and to adjust porosity. The more porous, the greater extensibility and less rigidity the wall shows. Once growth stops, the wall flexibility decreases and gives in to more strength, so wall shape is locked in place, while partial resilience is remained to buffer against turgor pressure.

Goals and challenges

Inherent complexity and heterogeneity

Scientists have been genetically engineering plants to optimize their utilization for decades. Most changes are achieved by altering wall-modifying enzymes, because the texture, digestibility, and appearance, are greatly influenced by cell wall properties. Many genes have been targeted, however, the resulting phenotypes are not always favorable or dramatic as expected. The structure and composition of cell walls are complicated and yet not completely characterized. Adjusting one enzyme and its products rarely impacts the plant tremendously. It seems that cell walls are adept at compensating for defects. The immobility of plants has forced them to evolve lines of defense and to adapt to severe external stimuli. As we understand more about plant cell walls, we will be able to manipulate plant traits to our desires more efficiently.

The plant cell wall varies among species and tissues, during growth stages, and in response to stimuli. The amount of each component is not constant. Compositional data reflect the accumulated net outcome from all of these variables. Even around a single cell the wall is not homogeneous, the extracellular matrix is a mosaic of different cell wall architectures; there are zones of different structures, the middle lamella, thickenings, channels, and corners, where composites and their distribution differ for apoplast multifunction. The cultured arabidopsis cell line is a relatively simple, homogeneous system to study the generic model of primary wall structure. Research on specific tissues or transient stages can further elaborate wall structural models.

Trace amount, weighing great

Xyloglucan has been thought to non-covalently interact exclusively with cellulose for the last 40 years, however in the 1990s and 2000s, some of the xyloglucan was found to be strongly

associated with pectin. In fact in the first detailed tentative model of a cell wall, the reducing end of the xyloglucan chains were depicted as being covalently linked to arabinan sidechains of pectin by Keegstra, et al. Some of the xyloglucan extracted from cell walls with strong alkali was found to bind to anion exchange columns and co-eluted with acidic polysaccharides. Strong alkali, high voltage, 8M urea and proteinases all failed to interrupt the interaction. Isotopic tracing and tentative enzyme digestions suggested that the linkage might be through arabinan and/or galactan side chains of RG-I. The xyloglucan-pectin interaction is common in suspension-cultured angiosperm cells (Thompson 2000, W. D. Bauer 1973, Z. A. Popper 2005). However, the exact nature how xyloglucan is linked to RG-I has remained elusive. We broke the linkage by cleaving the XG-RG complex with endo-arabinanase (and/or endo-galactanase) instead of cutting up rhamnogalacturonan backbone. The resulting xyloglucan-oligoarabinans were heterogeneous and completely consisted of neutral sugars. The xyloglucan chains could range from 9 kD to >900 kD (Park 2015). Considering that up to 50% of XG and RG are covalently linked (Z. A. Popper 2008), the linkage is crucial for the structural model of the cell wall and for better explaining why significant change in pectin or xyloglucan do not affect the phenotype as expected (Cavalier 2008). One major obstacle to determining the nature of the linkage is that quantitatively it is probably only a tiny portion of the whole wall mass.

Enormous structural diversity with very similar building blocks

Here I present a brief discussion of the complexities of characterizing an oligosaccharide or polysaccharide. Monosaccharides even with the same molecular weight present many possibilities. They can be aldose or ketose, and various combinations of hydroxyl group spatial orientations determine which epimers, such as glucose or galactose, xylose or arabinose they are. Monosaccharides can be D- or L- enantiomers, such as D-glucose vs L-glucose. The same monosaccharide adopts different ring configurations to give rise to furanose or pyranose forms, and adopts different anomeric configurations of C1 to lead to alpha or beta anomers.

Monosaccharides are able to form glycosidic bonds at multiple different hydroxyls, leading to linear or bent connection between residues, resulting in straight or branched polymers. The structural permutations of a trisaccharide comprised only of hexoses are high, up to 38,016 (Laine 1997).

Advanced spectroscopic methods for determining the exact structure of an oligo- or polysaccharides are limited. Mass spectrometry is limited in revealing structural information, such as, D- or L-, furanose or pyranose, alpha- or beta- forms and linkage positions. 2D or 3D NMR spectroscopy can show all of these but chemical shifts of isomers are so close that there is severe overlap of signals and the sensitivity of NMR is way lower than that of mass spectrometry.

The key points, separation and characterization of the linkage, are extremely challenging. Even though we managed to trim the xyloglucan-oligoarabinan to smaller sizes with xyloglucan-specific endoglucanase (XEG), the digestion product was still a series of molecules consisting mostly of pentoses and hexoses. The mixture was oligomers of overlapping molecular weights and of very similar physicochemical features. Regular xyloglucan subunits with different side chains were mixed with xyloglucan subunits that have oligo-arabinan (and/or oligo-galactan) attached, which all made it extremely difficult to separate and distinguish the linkages. Arabidopsis cell culture was adopted, not only because of the easy maintenance, but due to the fucosylation of arabidopsis xyloglucan which greatly clarifies MS and NMR assignments. Without these deoxyhexose residues, the XEG digestion product would be all Hex_mPen_n, which are hard to differentiate from other neutral saccharide contaminants. Since deoxyhexoses such as fucose are much less common in other neutral wall components, they can be used to identify XG oligomers.

Here comes the technical dilemma, intact wall polymers span a wide range of physico-chemical features, and are too big to characterize; whereas digested fragments comprising

isomeric residues exhibit overlapping properties, and are too similar to distinguish. Thus in this dissertation, we combined multiple methods and procedures to profile the XG-pectin linkage.

CHAPTER II

METHODOLOGY

2.1 Arabidopsis thaliana cell culture

Arabidopsis cell suspension cultures were initiated by adding 3~4 g of callus (*Arabidopsis thaliana* cell line T87) to NT-1 liquid medium and shaken at 120 rpm under continuous light at 25 °C. After about 2 weeks (late logarithmic phase) cells were harvested with fine nylon cloth (37 μm mesh).

2.2 Cell wall preparation

Cell walls were prepared as described by Komalavilas and Mort (Komalavilas 1989). Harvested *Arabidopsis* cells were rinsed with 10 vol of 100 mM potassium phosphate buffer (pH 7.0) and then with 6 vol of 500 mM potassium phosphate buffer (pH 7.0). Filtered cells were resuspended in 1 vol of 500 mM potassium phosphate buffer (pH 7.0) and broken using a Polytron homogenizer (Brinkmann Instruments, NY) in an ice bath for 12 min (stopped every 3 min to cool down), the suspension was examined under a microscope to ensure the cells were cracked thoroughly. Homogenate was washed sequentially with 5 vol of 500 mM potassium phosphate (pH 7.0), 10 vol of distilled water, 5 vol of 1:1 methanol-chloroform (v/v), and then 10 vol of acetone. The acetone-insoluble residues were air dried and collected as cell walls.

2.3 Pre-treatment of cell walls with saponification and endopolygalacturonase

Dry cell walls were suspended in KOH (pH 12) to a final concentration of 10 mg/ml and stirred overnight at 4°C. Cell walls were neutralized with 1 N HCl and centrifuged at 13,200 g for 15 min, precipitates were washed twice with water and centrifuged. Saponified cell walls were then suspended in 50 mM ammonium acetate buffer (pH 4.8) to ~10 mg/ml, and digested by endopolygalacturonase [cloned from *Aspergillus nidulans* ORF AN 8327.2 and expressed in *Pichia pastoris* (S. V. Bauer 2006), 0.1 U enzymes per 1 mg substrates], shaken at 90 rpm for 12 h at 37°C. Precipitates were collected by centrifuging at 13,200 g for 20 min, washed with water twice, and then lyophilized.

2.4 Extraction of xyloglucan-pectin complex with strong alkali

Dry pre-treated cell walls were suspended in 24% KOH (containing 0.1% $NaBH_4$ w/v) to ~10 mg/ml, and stirred gently overnight at room temperature. The suspension was centrifuged at 13,200 g for 25 min, precipitates were washed with KOH (pH 12) twice and centrifuged again. Supernatants were combined, neutralized with glacial acetic acid, and then desalted by dialyzing against water using dialysis membrane with a molecular weight cutoff of 12-14 kD (Spectrum Laboratories, Inc., CA). Dialyzed alkali extracts were collected and freeze-dried.

2.5 Anion exchange chromatography

Neutral saccharides and acidic saccharides were separated using a Dionex CarboPac PA1 anion exchange column (9×250 mm & 22×250 mm, Thermo Fisher Scientific, MA). Saccharides were dissolved in 30 mM ammonium acetate buffer (pH 5.2) to a concentration of ~10 mg/ml, and injected into PA1 column. Samples were eluted at 2 ml/min (for 9×250 mm column) or at 5 ml/min (for 22×250 mm column), using a multi-step gradient of pH 5.2 ammonium acetate (0-6 min: 30 mM; 6-60 min: 30 mM-1 M; 60-70 min: 1 M-2 M; 70-80 min: 2 M; 80-90 min: 2 M-30

mM). Eluted fractions were monitored with a Sedex55 evaporative light-scattering detector (S.E.D.E.R.E, France).

2.6 Enzymatic digestions

Xyloglucan can be hydrolyzed into signature repeating subunits with the catalysis of xyloglucanase (or xyloglucan-specific endoglucanase, XEG) from *Paenibacillus sp.*, GH5 (Megazyme). Xyloglucan-containing samples were dissolved in 50 mM ammonium acetate buffer (pH 5.2) to ~10 mg/ml, reactions were started by adding xyloglucanase (0.02 U per 1 mg of substrate), and were allowed to proceed at 37°C for 1 h.

Sugars were dissolved in 50 mM ammonium acetate buffer (pH 5.2) to ~10 mg/ml, and hydrolyzed with different enzymes. α-L-arabinosidase [cloned from Aspergillus nidulans ORF AN1571.2 and expressed in Pichia pastoris (S. V. Bauer 2006)] digestion was performed at 65°C for 1 h (0.12 U per 1 mg substrate). Endo-(1,5)-α-L-arabinanase [cloned from Thermotoga petrophila ORF Tpet637.1 and expressed in Escherichia coli (F. M. Squina 2010)] digestion was performed at 80°C for 10 h (0.015 U per 1 mg substrate). Endo-β-(1,4)-galactanase A [cloned from Emericella nidulans ORF AN5727 (S. V. Bauer 2006)] digestion was performed at 37°C for 1 h (0.1 U per 1 mg substrate).

2.7 Capillary zone electrophoresis (CZE)

The aldehyde groups at the reducing ends of carbohydrates were derivatized by reductive amination with negatively charged fluorophore 8-aminonaphthalene-1,3,6-trisulfonic acid (ANTS) or 8-aminopyrene-1,3,6-trisulfonic acid (APTS) using $NaBH_3CN$ as the reducing agent.

Polysaccharides were dissolved in ddH_2O to ~10 mg/ml, then mixed with 0.5 vol of $NaBH_3CN$ (1 M in DMSO) and 5 vol of ANTS (23 mM in 3% acetic acid w/v). The mixture was then heated at 80°C for 1 h. Derivatized samples were analyzed on a custom-built CZE system

consisting of a 355 nm UV diode-pumped solid-state (DPSS) laser and a fused-silica capillary (50 cm × 50 μm i.d., Polymicro Technologies, AZ). Electrophoresis was conducted under 18 kV, in sodium phosphate running buffer (0.1 M, pH 2.5) with the cathode at the inlet (A. J. Mort 2020) .

If using APTS, 1~10 vol of carbohydrate solution (10 mg/ml) was mixed with 10 vol of $NaBH_3CN$ (1 M in DMSO) and 0.5 vol of APTS (0.2 M in 25% acetic acid v/v), mixture was heated at 80°C for 1 h. Derivatized samples were analyzed on capillary zone electrophoresis Biofocus-2000 system (Bio-Rad laboratories, CA) which was equipped with a fused-silica capillary (31 cm × 50 μm i.d., Polymicro Technologies, AZ) and argon-ion laser (448 nm excitation). A voltage of 15 kV was applied to separate APTS-labeled molecules using sodium phosphate running buffer (0.1 M, pH 2.5) with the cathode at the inlet, 1 M NaOH was used to thoroughly clean the capillary between runs (A. J. Mort 2020).

Carbohydrates reductively labeled with uncharged fluorescence 2-aminobenzamide (2-AB) were examined with the custom built CZE system equipped with a 355 nm DPSS-laser and a fused-silica capillary (87 cm × 50 μm i.d., Polymicro Technologies, AZ). 10 vol of polysaccharides solution (~10 mg/ml in ddH_2O) was mixed with 2 vol of $NaBH_3CN$ (1 M in DMSO) and 8 vol 2-AB (0.35 M in 30% acetic acid/DMSO v/v), then heated at 80°C for 2 h. (Pabst 2009). Derivatized samples were run at 20 kV in sodium phosphate running buffer (50 mM, pH 6.7, containing 150 mM SDS) with anode at the inlet (Tran 1998).

Table 2.1 Fluorescent labeling of reducing sugars:

Labeling reagent	Structure	Labeled product	λ_{ex}, nm	λ_{em}, nm	M.W.(Da)	Labeling procedures
8-Aminopyrene-1,3,6-trisulfonic acid (APTS)	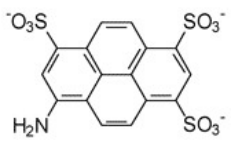	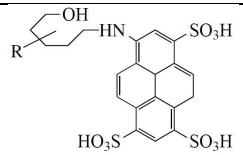	488	520	457.45	10-100 µg sample, +10 µl NaCNBH3 (1 M in DMSO), +0.5 µl APTS (0.2 M in 25% HAc/H_2O), 80°C for 1 h. (Mort, et al, 2020)
8-Aminonaphthalene-1,3,6-trisulfonic acid (ANTS)	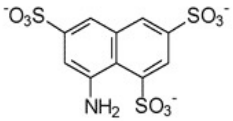	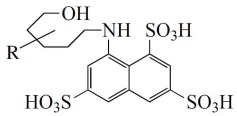	353	535	383.37	20 µg sample (in 2 µl H_2O), +1 µl $NaCNBH_3$ (1 M in DMSO), +10 µl ANTS (23 mM in 3% HAc/H_2O), 80°C for 1 h. (Mort, et al, 2020)
5-Aminonaphthalene-1-sulfonic acid (5AN1S)	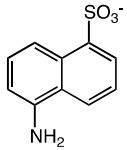	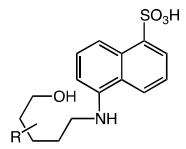	325	-	223.25	20 µg sample (in 2 µl H_2O), +1 µl $NaCNBH_3$ (1 M in DMSO), +10 µl 5AN1S (100 mM in 30% HAc/DMSO), 80°C for 1 h.
5-Aminonaphthalene-2-sulfonic acid (5AN2S)	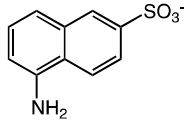	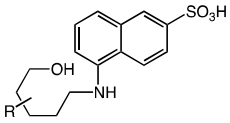	325	460±40 (Ma 2005)	223.25	20 µg sample (in 2 µl H_2O), +1 µl $NaCNBH_3$ (1 M in DMSO), +10 µl 5AN2S (100 mg/ml, in 1 N NH_4OH), 80°C for 1 h.
2-Aminobenzamide (2-AB)	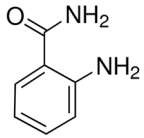	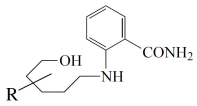	356	450	136.15	100 µg sample (in 10 µl H_2O), +2 µl $NaCNBH_3$ (1 M in DMSO), +8 µl AB (0.35 M in 30% HAc/DMSO), 80°C for 2 h. (Pabst, et al, 2009; Shilova, et al, 2003)

2.8 Sugar composition determined by gas chromatography

100 μg dry samples and 100 nmol internal standard of inositol were placed in glass vials with Teflon-lined and screw caps, 200 μl methanolic HCl (1.5 N) and 50 ul methyl acetate were added to methanolyze the samples. Vials were sealed and heated at 80°C for 3 h, and then cooled down. A few drops of *t*-butanol was added to each vial, and the mixtures were evaporated to dryness under nitrogen. 50 μl of trimethylsilylating reagent [5:1:1 anhydrous pyridine (Sigma-Aldrich Inc, USA) : hexamethyldisilazane (Sigma-Aldrich Inc, USA): chlorotrimethylsilane (Alfa Aesar, England)] was added to each dried sample vials and allowed to react for 15 min at room temperature. The derivatized samples were evaporated to just dryness under nitrogen, and dissolved in 100 μl iso-octane. 1 μl of derivatized sample was injected and separated on a fused-silica capillary column (30 m × 0.25 mm i.d., Durabond-1 liquid phase, J&W Scientific, Inc., USA) installed in a Varian 3300 & 3350 (Sunnyvale, USA). Sample was injected at 105°C and held for 1 min, temperature was raised to 160°C at a rate of 10°C /min and held at 160°C for the next 4 min, the column temperature was then increased to 220°C at a rate of 2°C /min and then elevated to 240°C at a rate of 10°C /min. The column was kept at 240°C for another 10 min before resetting for the next injection. Chromatograph peaks were recorded and integrated on a custom integration program (LawsonPolled.2.6 constructed by Dr. Jerry Merz) (Komalavilas 1989). Peak areas were measured using Chrom.4.6 program.

2.9 Gel filtration chromatography

Carbohydrates were fractionated by size on a HiLoad 16/600 Superdex 75 column (16×600 mm, GE life sciences, USA) using 50 mM ammonium acetate (pH 5.2) as eluent, or separated on Toyopearl HW-40S (10×500 mm, Tosoh Corporation, Japan) using 50 mM ammonium acetate buffer (pH 5.2, containing 25% acetonitrile) as mobile phase. Flow rate was set to 1 ml/min for both columns, fractions of native sugars were monitored either by a Sedex55

evaporative light-scattering detector (S.E.D.E.R.E, France) or by a Shodex R1-71 refractive index detector (Shodex, Japan), fluorescence-derivatized samples were monitored with a Linear 200 UV-detector (Linear Instruments, USA)

2.10 Hydrophilic interaction chromatography, reversed-phase chromatography, porous graphitic carbon column

Native or 2-AB labeled neutral sugars were separated by hydrophilic interaction chromatography (HILIC). Samples were dissolved in small amount of water or 50% acetonitrile/water mixture, then injected into silica-based amino column Luna NH_2 (10×250 mm, Phenomenex, USA) or polymer-based amino column Shodex-NH2P-50 (10×250 mm, Shodex, Japan). Fractions were eluted with a gradient of increasing water from acetonitrile (both containing 0.1% formic acid) ratio at a flow rate of 2 ml/min, and monitored with a Sedex55 evaporative light-scattering detector (S.E.D.E.R.E, France) or Linear 200 UV-detector (Linear Instruments, USA).

Sugars were dissolved in water and fractionated on a reversed-phase column Nova-Pak C18 (3.9×150 mm, Waters, USA) or with porous graphitic carbon column HyperCarb (4.6×100 mm, Thermo Electron Corporation, USA) with increasing gradient of acetonitrile/water ratio (both containing 0.1% formic acid) at 1 ml/min. Eluants were examined with a Sedex55 evaporative light-scattering detector (S.E.D.E.R.E, France) or Linear 200 UV-detector (Linear Instruments, USA).

2.11 Mass spectrometry

Carbohydrates were permethylated when necessary, since mass spectrometry showed much lower detection limit for permethylated sugars. Approximate 100 μg of native or fluorescence-labeled saccharides were freeze dried in a 4-ml glass vial, then vigorously mixed

with 50 µl CH_3I and 50 µl NaOH-DMSO slurry (NaOH tablets were ground in anhydrous DMSO to 40 mg/ml), and incubated for 1 h at room temperature. The reaction was stopped by slowly adding 500 µl of ddH_2O in an ice bath. The product mixture was extracted with 1 ml chloroform; organic phase was washed with 2 ml of water for three times and dried with anhydrous Na_2SO_4 crystals until clear, then evaporated under nitrogen. Permethylated samples were dissolved in 40% methanol/water and stored at -20°C until use (Fernández 2007, Oursel 2017, Ciucanu 1984).

Matrix-Assisted Laser Desorption/Ionization-Time Of Flight (MALDI-TOF): Non-methylated samples were pre-desalted with HyperCarb micro column (4.6×100 mm) and dissolved in water to ~10 mg/ml, while permethylated samples were dissolved in 50% methanol/water to ~10 mg/ml. For positive mode MS, 2,5-dihydrozybenzoic acid (DHB, Sigma, USA) was dissolved in 65% methanol/water to 10 mg/ml as matrix, 0.25 µl sample and 0.25 µl matrix were mixed and spotted on a 96 well ×2 target plate (PerSeptive Biosystems, Inc., USA). 1~2 mM Na^+ were added to samples when necessary. 10 mg/ml maltodextrin was mixed with DHB to spot on the plate as standard for external calibration. Air-dried samples were analyzed on a Voyager-DE PRO (PerSeptive Biosystems, USA) in reflector mode with an accelerating voltage of 20 kV and a delay time of 300 ns.

Electro Spray Ionization-Liquid Chromatography-tandem Mass Spectrometry (ESI-LC-MS/MS): Samples were pre-desalted and concentrated with C18-ZipTips, non-methylated samples were dissolved in water to ~ 0.1 µg/µl; permethylated samples were dissolved in 40% methanol/water to ~ 0.1 µg/µl. Samples were analyzed on hybrid LTQ-Orbitrap XL mass spectrometer (Thermo Fisher Scientific, USA) equipped with an Eksigent NanoLC-2D chromatography system and a New Objectives PV-550 nano-electrospray ion source. Saccharides were injected and trapped in a 4-cm pre-column (75 µm i.d., packed with Magic C18 AQ, 5 µm) using 0.1% formic acid as eluent, then separated on an analytical column (20 cm × 75 µm i.d., packed with Magic C18 AQ, 3 µm, Bruker) at a flow rate of 250 nl/min. Mobile phase Qa was

aqueous phase (containing 0.1% formic acid and 1 mM NaOH) (Delaney 2001, Wuhrer 2009), mobile phase Qb was organic phase consisting 80% acetonitrile in water (both containing 0.1% formic acid). Non-methylated saccharides were separated using gradient: Qb percentage was raise from 0 to 50% in 60 min; permethylated saccharides were separated with gradient elution pattern: Qb percentage was started with 50% at 0 min, increased to 87.5% at 30 min, then to 100% at 60 min and kept at 100% for the next 10 min. All solvents used on mass spectrometry were MS-grade purity. The analytical column eluant was sprayed into the ion source and ions were analyzed by Orbitrap in positive mode. During each full-range FT-MS scan, data-dependent acquisitions were performed, the most intense ions in the full scan were analyzed via MS/MS in the Orbitrap, peaks repeatedly shown as most intense in full scans within 50 sec were dynamically excluded for 90 sec. Spectra were collected and processed using Xcalibur 3.0 software (Thermo Scientific), the mass/charge ratios of ions were calculated with GlycoWorkBench 2.1.

2.12 Nuclear magnetic resonance spectroscopy

Samples were dissolved in 99.9% D_2O (Sigma–Aldrich, MO). ^{1}H NMR and TOCSY, COSY, HMBC, HMQC, and NOESY spectra were recorded at 21°C on a Varian Unity Inova 600 NMR spectrometer using Varian VNMRJ software. Proton decoupled ^{13}C NMR spectra (HMQC and HMBC) were recorded using a Varian 5 mm CHN triple resonance probe at 150.82 MHz. Total correlation spectroscopy (TOCSY) experiments were performed with a mixing time of 100 ms. All spectra used pre-saturation mode to suppress the water peak with saturation power at -9 (A. J. Mort 2013). Spectra collected from Bruker Neo 800MHz NMR were conducted at 298K using CP TCI Cryoprobe, recorded by Topspin 4.0 software, and processed by Mnova 10.0.1. Experiments on Bruker were performed with a relaxation delay of 1 sec, TOCSY mixing time of 80 ms and pre-saturation power PLW9=1.0 e^{-5} W.

CHAPTER III

RESULTS & DISCUSSION

3.1 Extraction and purification of XG-pectin complex from Arabidopsis suspension culture cell walls

Fresh *Arabidopsis thaliana* cells were collected, rinsed and homogenized to break up cell walls. The homogenate was washed with phosphate buffer and methanol-chloroform to remove lipids and proteins. The remainder, insoluble in both aqueous and organic solvents, was mostly cell wall polysaccharides.

Lyophilized cell wall polysaccharides were pre-saponified before endopolygalacturonase (EPG) digestion, since the affinity and reaction rate of endopolygalacturonase from different sources were found to be significantly affected by the distribution pattern and degree of methyl esterification of galacturonic acid residues in the substrate (Serrat 2004, Bonnin 2002, Daas 2000). Saponified cell walls were then hydrolyzed by EPG to solubilize homogalacturonan (HG) and release most of the rhamnogalacturonan II (RG-II) (Table 3.1).

Pre-treated cell walls were subjected to strong alkali, which can break the extensive hydrogen bonding between hemicellulose and cellulose. Cellulose remains insoluble after strong alkali treatment. Strong alkali extracts were neutralized and centrifuged. Part of the alkali extract

.

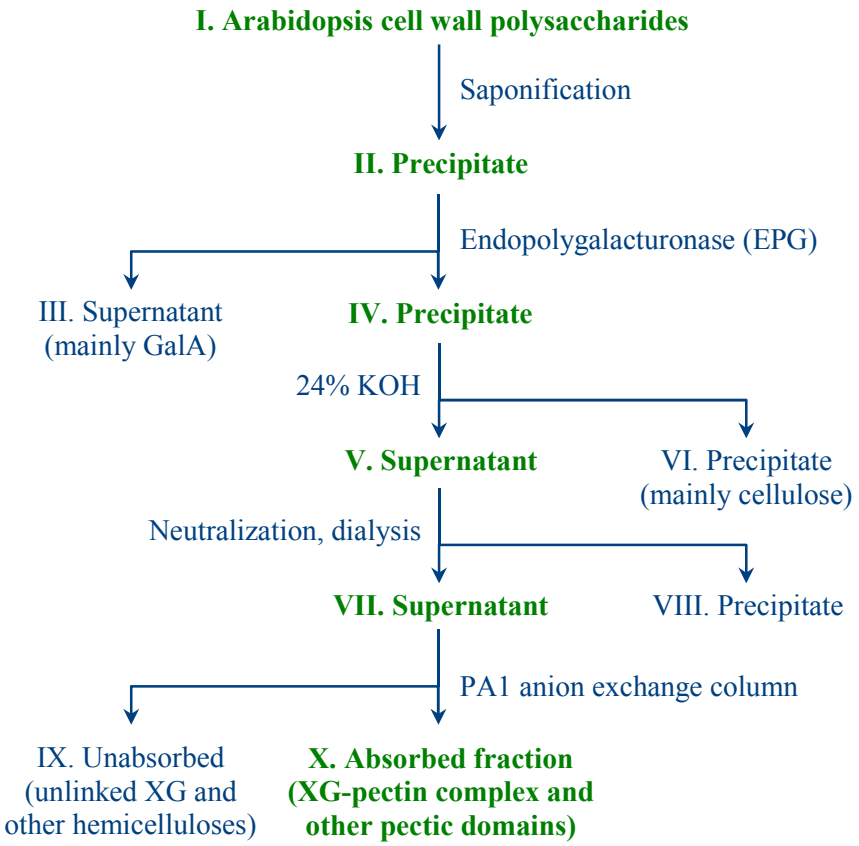

Figure 3.1 Experimental flowchart of extracting XG-pectin complex from lyophilized cell wall polysaccharides.

can only dissolve at pH>9 and precipitates when neutralized (Figure 3.1). Aliquots of products after each treatment were methanolyzed, derivatized, and analyzed with gas chromatography. Sugar residue compositions were then calculated (Table 3.1).

An aliquot of each product was hydrolyzed with xyloglucan-specific endoglucanase (XEG), enzyme digested products were derivatized with ANTS, and analyzed by capillary zone electrophoresis (CZE) to detect the presence of xyloglucan (Figure 3.2), using ANTS-labeled cotton xyloglucan subunits as standard. Xyloglucan was successfully extracted by strong alkali

Table 3.1 Sugar compositions of intermediate products during extraction

MOLE%	Ara	Rha	Fuc	Xyl	GalA	Gal	Glc
I. Whole cell wall polysaccharides	22.1	9.7	1.5	12.9	34.9	9.6	9.2
II. Saponified cell wall pellet	20.9	12.2	1.7	10.9	37.6	13.1	3.5
III. EPG supernatant	17.1	7.5	0.4	3.4	58.5	10.0	3.1
IV. EPG pellet	25.6	8.9	2.0	13.6	31.5	12.8	5.7
VI. Alkali pellet	14.2	7.3	1.7	10.0	13.1	13.4	40.5
VII. Neutral-soluble alkali extract	25.0	10.5	2.8	21.8	17.2	11.0	11.8
VIII.Neutral-insoluble alkali extract	31.9	11.4	3.0	18.5	11.7	14.7	8.7

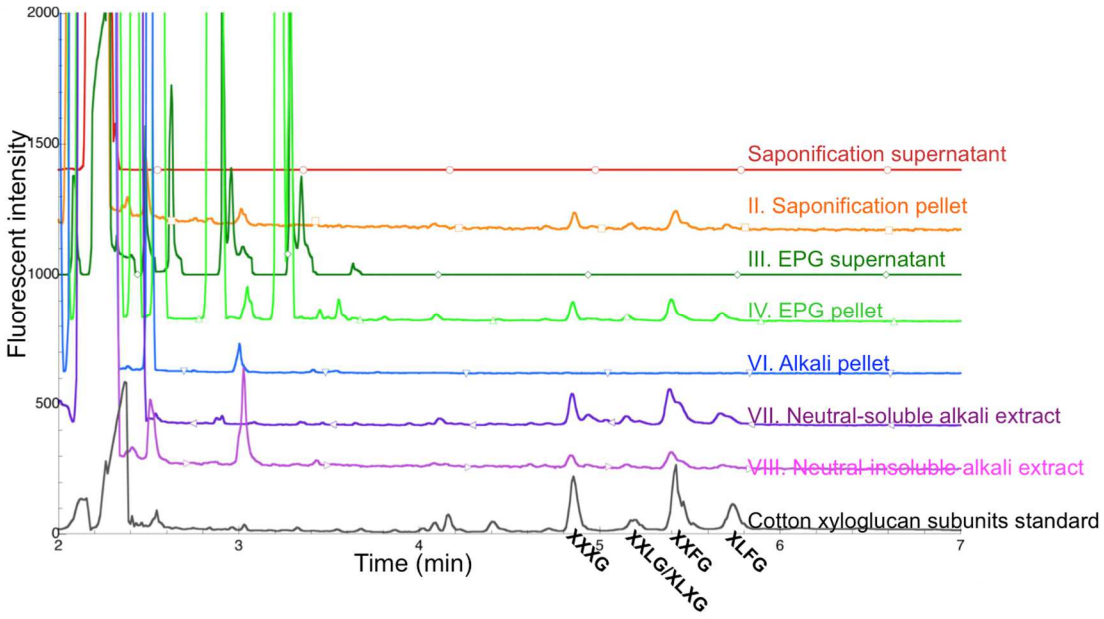

Figure 3.2 Xyloglucan presences during each step of treatment were tracked by XEG digestion and CZE.

and not detected in the alkali-treated residue. After neutralization and dialysis, there was also noticeable amount of xyloglucan in the neutral-insoluble alkali extract.

Neutral-soluble alkali extracts were separated by PA1 anion exchange HPLC column, non-charged polysaccharides were washed through the column first with low salt buffer (peak 1,

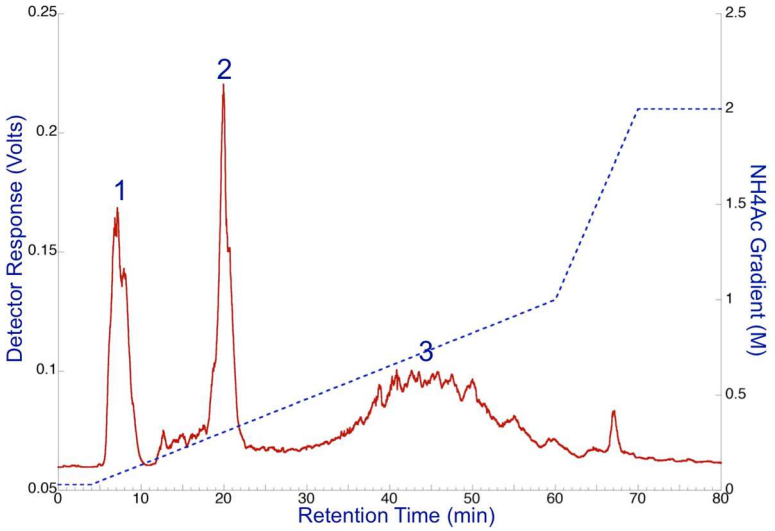

Figure 3.3 Alkali extracts were separated on PA1 anion exchange column. Eluting gradient was displayed in dashed line.

Table 3.2 Sugar compositions of PA1 separated alkali extracts

MOLE%	ARA	RHA	FUC	XYL	GALU	GAL	GLC
Peak1	6.9	n.d.	6.3	41.3	n.d.	14.1	31.4
Peak2	21.3	n.d.	1.1	61.9	0.8	6.2	8.6
Peak3	30.1	15.6	2.2	14.0	16.8	16.2	4.9

* n.d.: not detected

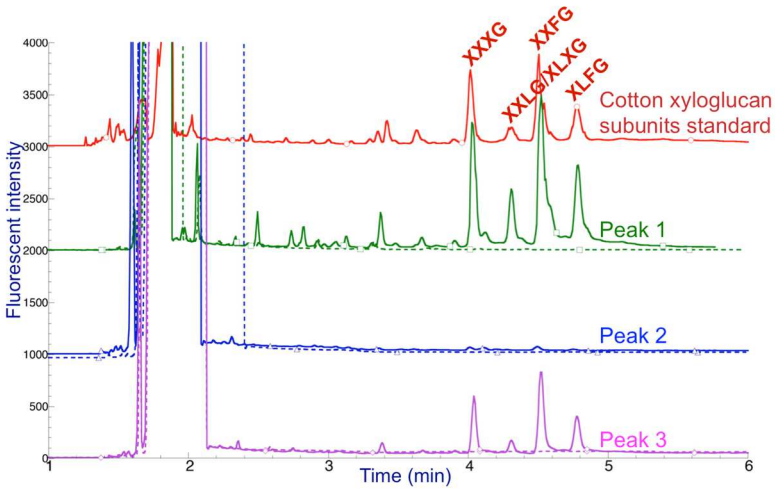

Figure 3.4 CZE detected xyloglucan presences in each fraction isolated by PA1 column. Dashed lines were samples without XEG treatment, solid lines were XEG digestions.

Figure 3.3). Xyloglucan-pectin complexes were rich in GalA residues and negatively-charged requiring a much higher ion strength to elute from the PA1 column (peak 3 Figure 3.3). An aliquot of each peak was examined by GC (Table 3.2) and CZE (Figure 3.4). Peak 2 was mostly salts and barely contained any acidic sugars, it was likely to be other hemicelluloses i.e. xylan or arabinoxylan due to its high molar percentage of xylose and arabinose (Table 3.2). Also from the electropherograms (Figure 3.4), xyloglucanase could hardly release any xyloglucan subunits from peak 2, while xyloglucans were mostly found in the flow-through fraction (peak 1) and in high-salt elution fraction (peak 3). From the sugar compositions, the flow-through fraction (peak 1) was mainly composed of non-charged free xyloglucan and other hemicelluloses that were extracted by strong alkali, and the elution fraction (peak 3) was comprised of covalently linked xyloglucan-pectin and other pectic polysaccharides. The pectin backbones were of different lengths and contained different amounts of negatively charged uronic acid residues, thus peak 3 was continuous and wide.

3.2 Isolation of native linkage between XG and pectin

3.2.1 Isolating XG-pectin linkage by trimming pectin first

Pectin-bonded xyloglucan was separated from free xyloglucan by a PA1 anion exchange column, yet this PA1-adsorbed fraction was still mixed with other pectic polysaccharides (peak 3 in Figure 3.3 or Fraction X in Figure 3.1). To isolate xyloglucan with linkage from the XG-pectin complex mixture, specific enzymes that can break the arabinan linkage were used.

The α-(1,5)-L-arabinan side chains of RG-I were highly branched. To decrease steric hindrance and give better access to the backbones of the arabinan, the XG-pectin complex mixture was first subject to α-L-arabinofuranosidase (AN1571, expressed in Pichia pastoris) which can remove terminal L-arabinofuranoses from non-reducing ends and expose the backbones of arabinans. The arabinosidase-hydrolyzed product was purified on a PA1 column (Figure 3.5).

About half of the flow-through fraction (peak 4, Figure 3.5) was arabinose digested from the XG-pectin complex (Table 3.3). After freeze-dry concentration, there was only a little sugar

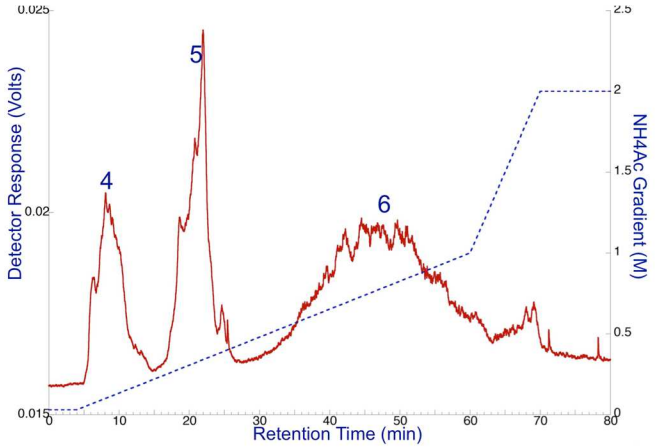

Figure 3.5 Arabinosidase-hydrolyzed product separated on PA1 anion exchange column. Eluting gradient was displayed in dashed line.

Table 3.3 Sugar compositions of PA1 separated arabinosidase product

MOLE%	ARA	RHA	FUC	XYL	GALU	GAL	GLC
Peak4	54.2	0.6	2.8	19.9	n.d.	8.0	14.5
Peak5	20.5	4.4	1.5	53.7	5.1	9.0	5.8
Peak6	17.0	15.9	2.2	12.5	28.0	18.3	6.0

* n.d.: not detected

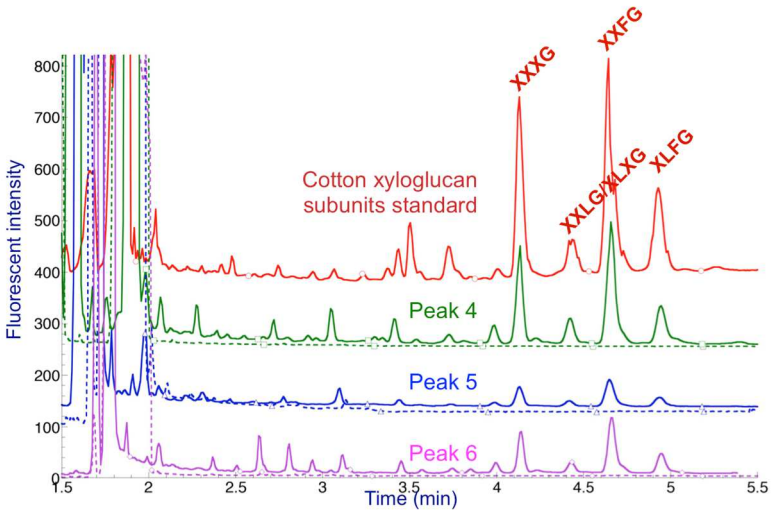

Figure 3.6 CZE detected xyloglucan presences in PA1 separated arabinosidase product. Dashed lines were samples without XEG treatment, solid lines were XEG digestions.

left in peak 5. The sugar composition indicted the presence of xylan and/or arabinoxylan and little amount of pectin. Aliquots of all three peaks were digested with xyloglucanase and analyzed on CZE (Figure 3.6). Xyloglucan was detected in each peak fraction, which was unexpected for the flow-through fraction (peak 4). The xyloglucan that co-eluted with pectin was more likely to be covalently linked, since harsh treatment like molars of strong alkali could not even separate them. Arabinosidase was an exo-hydrolase, which was not expected to enzymatically cleave xyloglucan from XG-pectin complexes. To further investigate this, a small amount of XG-pectin complex mixture (fraction X, 20 mg) was incubated at 80°C without any enzyme, and then separated on a PA1 column (Figure 3.7).

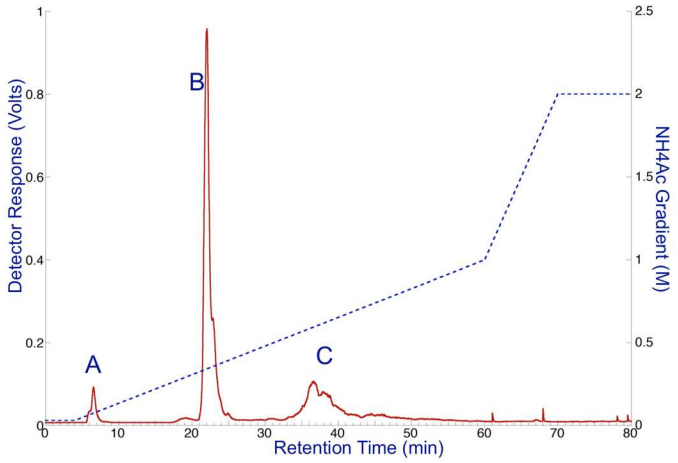

Figure 3.7 80°C-incubated product separated on PA1 anion exchange column. Eluting gradient was displayed in dashed line.

Table 3.4 Sugar compositions of PA1 separated 80°C-incubated product

MOLE%	Ara	Rha	Fuc	Xyl	GalA	Gal	Glc
Peak A	16.3	2.4	6.0	37.7	n.d.	12.7	24.9
Peak B	23.8	5.8	1.5	51.9	2.0	8.4	6.6
Peak C	26.7	17.0	1.9	10.4	22.8	16.1	5.2

* n.d.: not detected

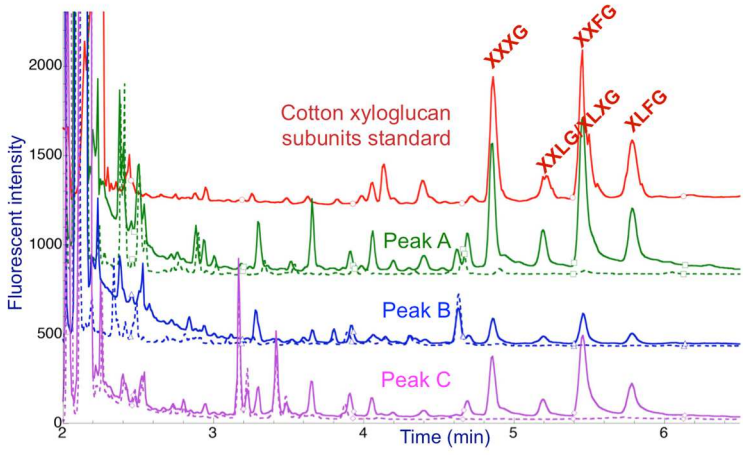

Figure 3.8 CZE detected xyloglucan presences in PA1 separated 80°C-incubated product. Dashed lines were samples without XEG treatment, solid lines were XEG digestions.

Like with the arabinosidase digestion product, xyloglucan was detected in the flow-through, the PA1 lightly bound fraction, and the PA1-bound fraction (Peak A, B, and C, Figure 3.8). From Table 3.3 and Table 3.4, molar percentage of arabinose was remarkably higher in arabinosidase-released neutral sugars (54.2% in Peak 4), while the sugar composition of other sugar residues were of similar ratio with the flow-through fraction released by 80°C incubation (Peak A). Molar ratios were similar in PA-bound fractions between different treatments, sugar compositions were comparable except for arabinose percentage.

Strong alkali broke the extensive hydrogen bonds between xyloglucan and cellulose to solubilize the xyloglucan, however the following separation and purification could not be conducted under such extreme pH conditions, thus matrix polysaccharides solubilized by alkali had to be neutralized first. Part of the xyloglucan-containing component visibly precipitated at neutral pH. This indicated that non-covalent interactions may exist between polysaccharides, which even affected their solubility in aqueous solution. Arabinosidase and arabinanase both require higher temperature to react (65°C and 80°C), the heating may break some nonspecific binding between molecules by disturbing the hydrogen bonds or van der Waals interactions. The conformations of molecules might also be altered during heat incubation, which might make the nonspecific binding irreversible after cooling down.

Although there still might be xyloglucan non-covalently entangled in the XG-pectin complexes, the covalently linked complexes should remain in the PA1-bound fraction after arabinosidase (Peak 6, Figure 3.5). This fraction was then hydrolyzed by endo-(1,5)-α-L-arabinanase (Tpet 637.1, expressed in E.coli), and separated on a PA1 column (Figure 3.9).

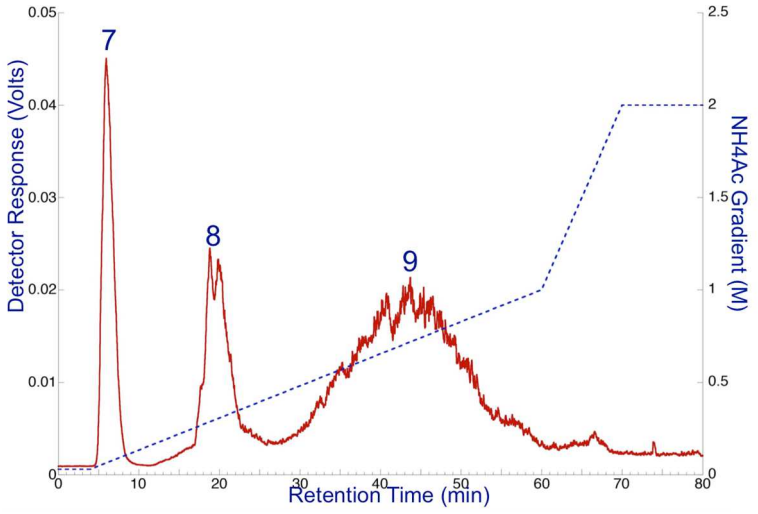

Figure 3.9 PA1-absorbed fraction of arabinosidase digestion was hydrolyzed with arabinanase (Tpet637) and separated by PA1 anion exchange chromatography. Eluting gradient was displayed in dashed line.

Table 3.5 Sugar compositions of PA1 separated arabinanase product

MOLE%	Ara	Rha	Fuc	Xyl	GalA	Gal	Glc
Peak7	36.0	1.4	3.4	33.8	0.5	9.8	15.1
Peak8	34.7	10.6	1.6	28.0	7.0	11.1	7.0
Peak9	8.1	21.6	2.0	15.4	29.8	17.6	5.5

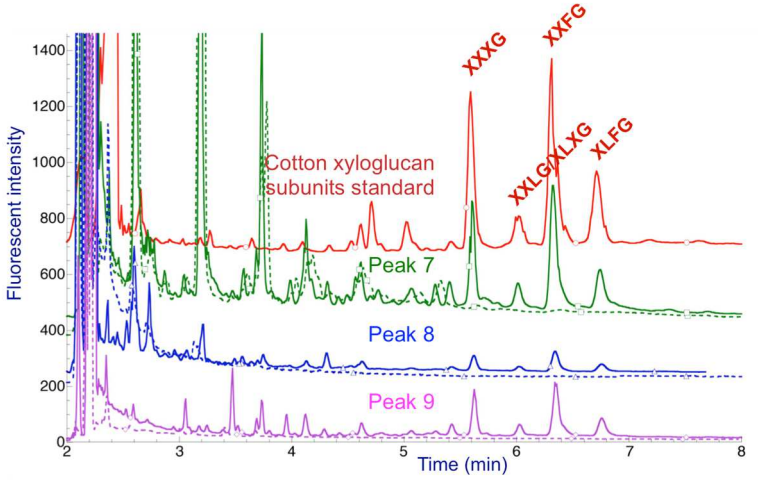

Figure 3.10 CZE detected xyloglucan presences in PA1 separated arabinanase product. Dashed lines were samples without XEG treatment, solid lines were XEG digestions.

Xyloglucan was found in all three peaks (Figure 3.10). The molar ratio between xylose and glucose residues is supposed to be ~3:4 in xyloglucan molecules. In PA1-unbound fraction (peak 7) there were a lot more xylose residues (33.8%, molar percentage) than glucose (15.1%), which indicated the existence of other neutral hemicelluloses like xylans and/or arabinoxylans, those hemicelluloses including some of xyloglucans might be stripped nonspecifically by heat like previously tested (Figure 3.7). Arabinanase trimmed xyloglucans should be also in this fraction, to analyze the linkage, it need to be further purified by separating the neutral flow-through (peak 7) on a Superdex-75pg size exclusion column (Figure 3.11). Monomers and dimers of tamarind xyloglucan subunits (1~3 kD) and arabinogalactan (~10 kD) were injected in the column as external standards.

The first peak isolated by Superdex-75pg (peak 10) was freeze-dried but left no visible residue, GC could not detect sugar presence in it either. The low molecular weight (LMW) fraction (peak 13) was mostly arabinoses (Table 3.6). CZE and MALDI-TOF MS analysis showed oligomers of pentoses (Figure 3.12 and 3.13.A), which indicated that the LMW peak

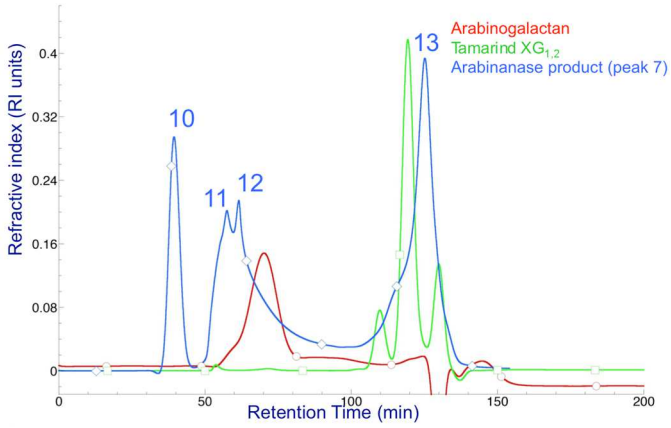

Figure 3.11 Arabinanase(Tpet637) released neutral fraction was separated on a Superdex- 75pg column (blue line, diamond mark). Red line (round mark) was arabinogalactan (~10 kD), green line (square mark) was monomers and dimers of tamarind XG subunits.

Table 3.6 Sugar compositions of Superdex-75pg separated product

MOLE%	Ara	Rha	Fuc	Xyl	GalA	Gal	Glc
Peak 11	2.3	0.5	9.2	44.9	0.5	16.3	26.2
Peak 12	6.6	0.8	5.8	52.4	1.3	13.9	19.0
Peak 13	69.1	3.2	1.0	9.1	0.7	8.7	8.3

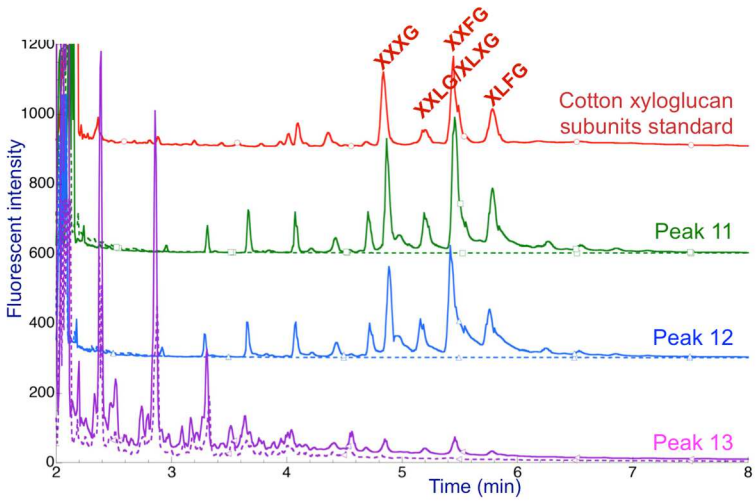

Figure 3.12 CZE detected xyloglucan presences in Superdex-75pg separated product. Dashed lines were samples without XEG treatment, solid lines were XEG digestions.

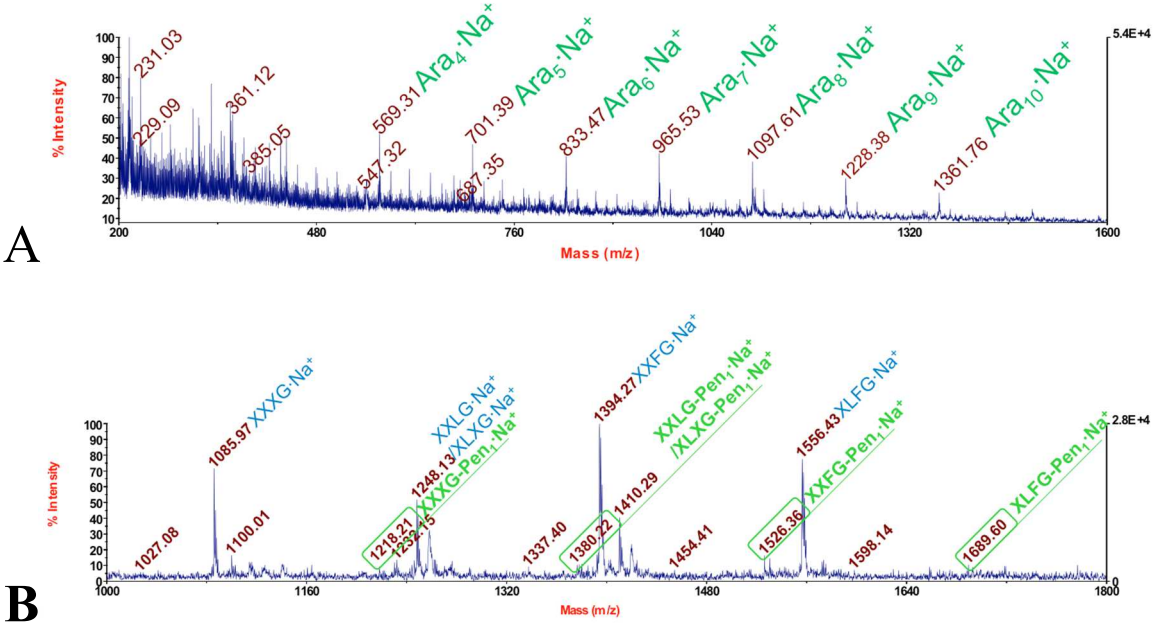

Figure 3.13 (A) Low molecular weight product (Peak 13) and (B) XEG digested bigger molecular weight product (Peak 12) of Superdex-75pg separation were analyzed with MALDI-TOF MS.

was mostly oligo-arabinans that were released by arabinanase (Tpet637.1). The xyloglucans were easily detected in peak 11 and 12 (Figure 3.12), which were eluted earlier than the arabinogalactan ~10 kD (Figure 3.11). We estimate that the xyloglucan chains were >10 subunits long. The arabinose residues detected in these higher molecular weight fractions were likely to be covalently bound to xyloglucans. To investigate this, peak 11 and 12 were digested with xyloglucanase and analyzed on MALDI-TOF MS (Figure 3.13.B)

In xyloglucanase hydrolyzed higher molecular weight peak (peak 12), after each xyloglucan subunit, there were traces of ions with one more pentose residue (Figure 3.13.B). XXXG, XXLG, and XLXG subunits contain only pentose and hexose residues. There might be isomers, such as other hemicelluloses, sharing the same m/z, so peaks with m/z of 1218.21, 1380.22 were not convincing enough to prove the presence of an extra pentose as a linkage remnant. Fucosylated subunits XXFG and XLFG were chosen as the indicators to see if there was additional arabinose residues covalently attached to them, since deoxy-hexose (ie. fucose) is relatively unusual in other neutral polysaccharides of arabidopsis cell walls. It is notable that potassiated deoxy-hexose has the same m/z as a sodiated hexose, so 1~2 mM Na^+ were added during sample treatment to maximize sodiated peaks while suppressing the potassiated peaks. In Figure 3.13.B, the peak with m/z of 1526.36 was 132 units bigger than XXFG·Na^+ (m/z 1394.27), and the peak with m/z of 1689.60 was 133 units bigger than XLFG·Na^+ (m/z 1556.43). The m/z value of pentose residue is 132, this extra pentose was very likely to be the arabinose linkage. (Calculated theoretical m/z: XXFG·Na^+ 1393.45, XXFG-Ara_1·Na^+ 1525.49, XLFG·Na^+ 1555.50, XLFG-Ara_1·Na^+ 1687.54. The observed m/z difference between Ara_9·Na^+ and Ara_{10}·Na^+ was also 133, such deviation from theoretical was possibly caused by MS calibration). That the intensity ratio between m/z 1394.27 and m/z 1526.36 was close to 10:1 fits with the higher molecular weight product being >10 xyloglucan subunits long. We suggest that linkages between xyloglucan-pectin are on the reducing ends of xyloglucan chains. Peak 11 showed a similar mass

spectrum pattern as peak 12, only the intensities of xyloglucan subunits with an extra pentose were even smaller (figure not shown).

To further rule out the possibility that the extra arabinose residue was on the side chain of xyloglucan, peak 12 (or peak 11) was derivatized using two different protocols for comparison of the reducing-end subunits with internal or non-reducing end subunits. When an aliquot of peak 12 was hydrolyzed with XEG first, then derivatized with ANTS, all subunits would have ANTS and show fluorescent signals in the electropherogram. If peak 12 (using ten times the amount to amplify the final fluorescent signals) was derivatized with ANTS first, then digested by xyloglucanase, only subunits at the reducing ends should have ANTS labels, while the other internal subunits or non-reducing end subunits should not be labeled and won't even migrate in the electric field at pH 2.5.

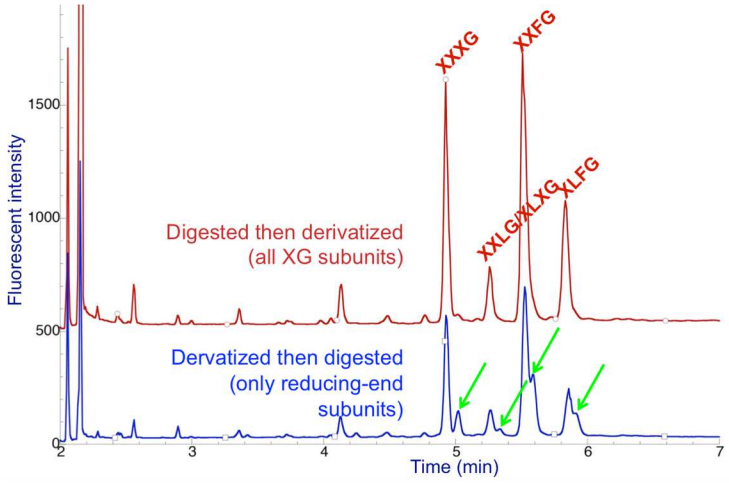

Figure 3.14 CZE detected xyloglucan presences in peak 12. Red line: all subunits were labeled with fluorophores, blue: only reducing-end subunits were labeled.

From the bottom panel in Figure 3.14, there were clearly side-peaks or shoulders (green arrows) after each xyloglucan subunit peak, which indicated that the arabinoses detected were attached to the reducing end subunit of xyloglucan. It was also notable that a significant amount

of the reducing ends (blue line) were without arabinoses, these were possibly xyloglucan released by heat as mentioned previously. ANTS-derivatized reducing ends of peak 12 were purified on an HW-40 column, and analyzed by MALDI-TOF MS, however, the amount of the desired fraction was too small and ANTS labeled sugars seem hard to ionize (data not shown).

Due to the limitation, as small final amount after multiple liquid chromatography operations, the intact XG-Ara_n complex we gained after arabinanase hydrolysis (Peak 12) was dissolved in D_2O and analyzed with 2D- heteronuclear NMR to determine how arabinose is linked to XG.

In the HSQC (heteronuclear single quantum coherence) spectrum (Figure 3.15), the cross peaks indicate the correlations between carbon atoms and directly attached protons. As indicated in figure 3.15 we could identify all of the signals for the anomeric carbons and protons expected in xyloglucans. There was a very weak signal corresponding to the C1-H1 of the reducing β-glucose. There were also two other signals in the anomeric region, one characteristic of an α-arabinofuranose. We found signature chemical shifts of L-Ara*f*, δ^1H around 4.15. (Table 3.7). In the HMBC (Heteronuclear Multiple Bond Correlation) spectrum (Figure 3.16), cross-peaks correspond to intra/inter-glycosidic scalar couplings from protons to carbons or from carbons to protons, the correlation could happen between atoms several covalent bonds apart. H4 of L-Ara*f* shows signature chemical shift at ~ 4.1 ppm, but none of the carbon atoms of an Ara has chemical shift close to ~102.3 ppm, only δC1 of 1,4-substituted Glc is close to 102.3 ppm. This cross peak indicated the inter-glycosidic correlation between H4 of Ara and C1 of reducing-end unbranched Glc possibly through C5 of Ara, this long-range interglycosidic coupling is often seen in HMBC experiment. The spectra are very crowded between 3~4 ppm, and the XG vs. Arabinan ratio is very big in intact XG-Ara_n product, it's hard to unambiguously assign the chemical shifts other than the anomeric region, the reducing end of XG is possibly 1,5 linked to the arabinan sidechain of RG-I.

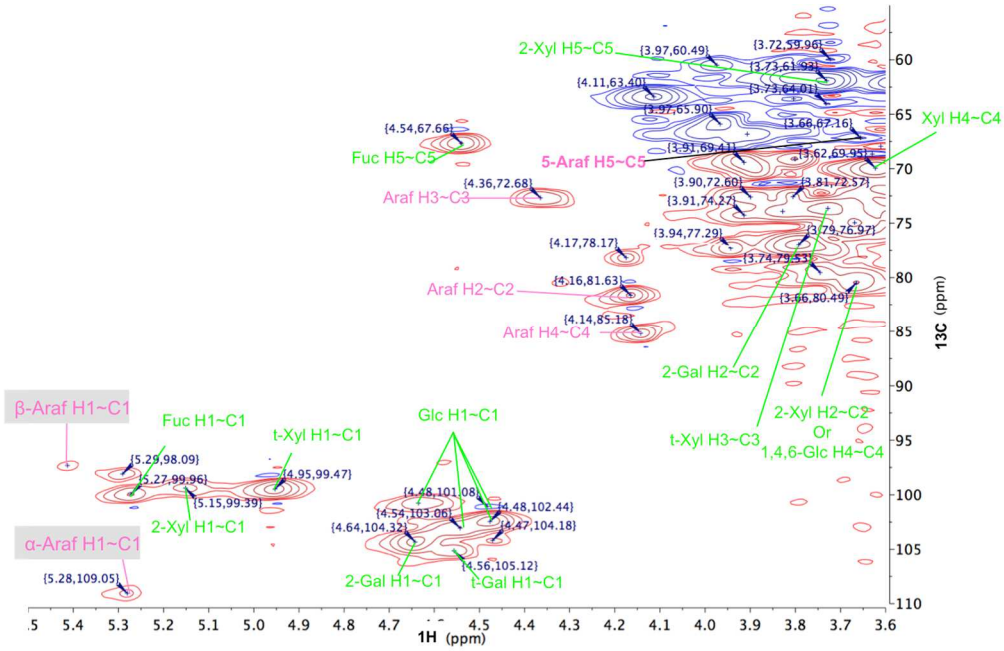

Figure 3.15 Selected regions of the HSQC (heteronuclear single quantum coherence) spectrum of XG-Ara$_n$ (Peak12).

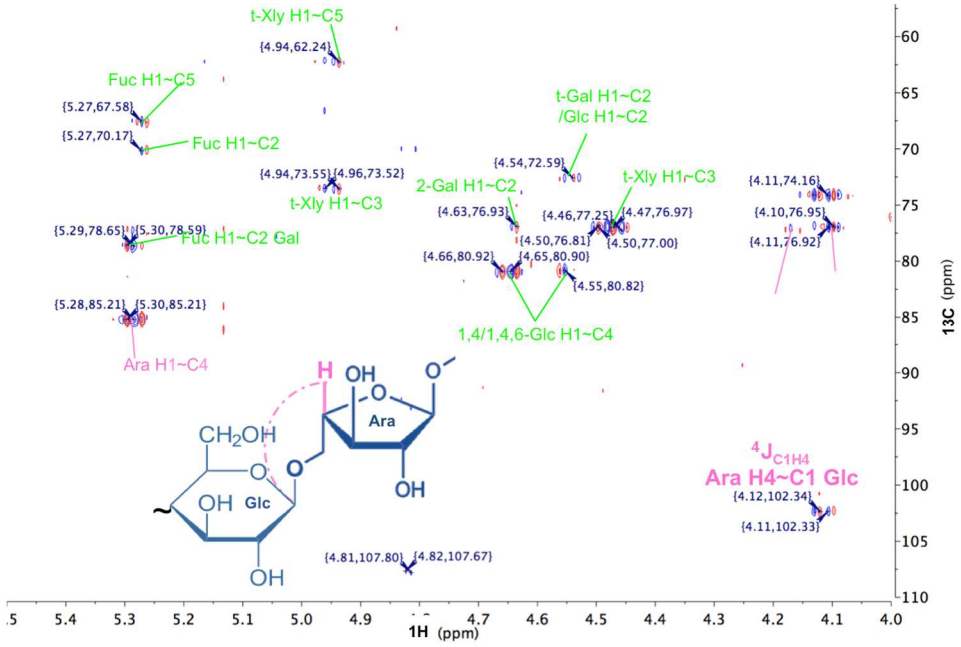

Figure 3.16 Selected regions of the heteronuclear multiple-bond correlation (HMBC) spectrum of XG-Ara$_n$ (Peak12).

Table 3.7 NMR assignments of XG-Ara$_n$ (Peak12)

Side Chain	Residue	H1	H2	H3	H4	H5ax, H5eq	H6, H6'
G	→4)-α-D-Glc*p*	5.29	n.a.	n.a.	n.a.	n.a.	n.a.
G	→4)-β-D-Glc*p*	4.64	n.a.	n.a.	n.a.	n.a.	n.a.
G	→4)-β-D-Glc*p*-(1→	4.54	3.40	n.a.	3.75	3.68	n.a.
X	→6)-β-D-Glc*p*-(1→	4.47	n.a.	n.a.	n.a.	n.a.	n.a.
X/L/F	→4,6)-β-D-Glc*p*-(1→	4.48	3.30	3.74	3.66	3.80	3.97, n.a.
X	α-D-Xyl*p*-(1→	4.95	3.55	3.73	3.62	3.58, 3.74	
L/F	→2)-α-D-Xyl*p*-(1→	5.15	3.66	n.a.	3.63	3.58, 3.73	
L	β-D-Gal*p*-(1→	4.56	n.a.	3.57	3.92	n.a.	n.a.
F	→2)-β-D-Gal*p*-(1→	4.64	3.79	n.a.	3.92	n.a.	n.a.
F	α-L-Fuc*p*-(1→	5.29	3.82	3.89	3.81	4.54	1.26
	→5)-α-L-Ara*f*	5.28	4.16	4.36	4.14	3.66, n.a	
	→5)-β-L-Ara*f*	5.29	n.a.	n.a.	n.a.	n.a.	

Residue	C1	C2	C3	C4	C5	C6
→4)-α-D-Glc*p*	98.09	n.a.	n.a.	n.a.	n.a.	n.a.
→4)-β-D-Glc*p*	100.76	n.a.	n.a.	n.a.	n.a.	n.a.
→4)-β-D-Glc*p*-(1→	103.06	73.37	n.a.	79.62	74.95	n.a.
→6)-β-D-Glc*p*-(1→	104.18	n.a.	n.a.	n.a.	n.a.	n.a.
→4,6)-β-D-Glc*p*-(1→	102.44	73.41	73.63	80.49	76.92	65.84
α-D-Xyl*p*-(1→	99.47	72.08	73.65	69.95	61.94	
→2)-α-D-Xyl*p*-(1→	99.39	80.49	n.a.	69.94	61.93	
β-D-Gal*p*-(1→	105.12	n.a.	74.1	69.4	n.a.	n.a.
→2)-β-D-Gal*p*-(1→	104.32	76.97	n.a.	69.4	n.a.	n.a.
α-L-Fuc*p*-(1→	99.96	70.51	72.58	70.14	67.66	16.51
→5)-α-L-Ara*f*	109.05	81.63	72.68	85.18	67.16	
→5)- β -L-Ara*f*	97.35	n.a.	n.a.	n.a.	n.a.	

Acetone in D_2O was chosen as internal reference: δ^1H=2.22ppm, $\delta^{13}C$=30.89ppm (Babij 2016).
n.a.: not assigned.

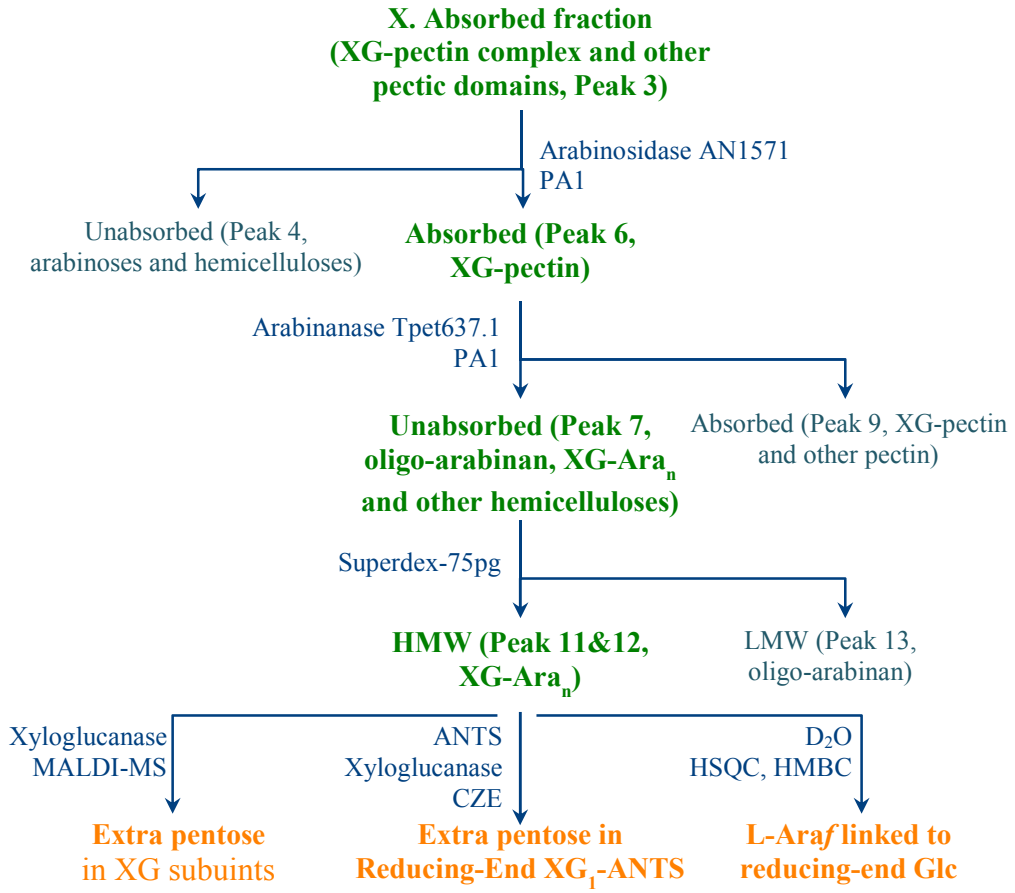

Figure 3.17 Experimental flowchart of isolating and analyzing XG-pectin linkage by trimming pectin first.

3.2.2 Quantitative analysis of XG-pectin degradation with enzymes

In LC-MS sugar samples were separated by liquid chromatography then ionized and analyzed with high-accuracy mass spectrometry. The chromatogram mass filter range can be set with specific m/z values (mass tolerance = ±5 mmu, millimass units in this research) to display the retention pattern of the desired polysaccharides. However it is difficult to define the mass filter range for the designated molecule with a calculated mass, because the ionization state of neutral sugars is complicated, sugar molecules are often sodiated or potassiated, which may lead

to wrong peak designation. For instance sodiated glucose has the same m/z (203) as potassiated fucose, since the mass differences between ^{23}Na & ^{39}K and between glucose (180 Da) & fucose (164 Da) are both 16 Da. Ionization with H^+, Li^+, NH_4^+, Na^+, K^+ and multiple charging further elevate the complexity. To avoid this, samples were dissolved and run in LC-loading solvent with additional 1 mM Na^+ to suppress other ions (Delaney 2001, Wuhrer 2009), and to favor cross-ring fragmentations in tandem MS (Rabus 2017, Cui 2001, Bythell 2017).

Aliquots of XG-pectin (peak 3) were digested with xyloglucanase then permethylated and separated on LC-MS (figure 3.18). Chromatograms were processed to show only five predominant xyloglucan subunits, five dark-colored chromatograms (left) were screened with most possible m/z values of each subunits, including singly-charged ions (z=1): $[M+H]^+$, $[M+Li]^+$, $[M+NH_4]^+$, $[M+Na]^+$, $[M+K]^+$, and doubly-charged ions (z=2): $[M+H+NH_4]^{2+}$, $[M+H+Na]^{2+}$, $[M+2NH_4]^{2+}$, $[M+NH_4+Na]^{2+}$, $[M+2Na]^{2+}$, other combinations or ions with more charge were rare when M<3kD, thus were not taken into consideration. Five pale-blue chromatograms (right) were LC screened with only sodiated ions: including: $[M+Na]^+$ and $[M+2Na]^{2+}$. M/z values were calculated with GlycoWorkBench 2.1 and shown in table 3.8. Filtered chromatograph peak areas were detected with Xcalibur Qual Browser and shown in the bottom rows of table 3.8, peak area is presumed to be proportional to molar concentration and used to estimate the amount of each analyte. Among ions of five permethylated xyloglucan subunits, more than 90% of each were sodiated, and the ratios were similar.

In the rest of the experiments, all LC-MS samples were dissolved and analyzed with addition of sodium ions, m/z values of only sodiated forms were used to process the LC chromatogram to display the desired peak, peak areas of sodiated ions were used to estimate the relative amount of the selected peak.

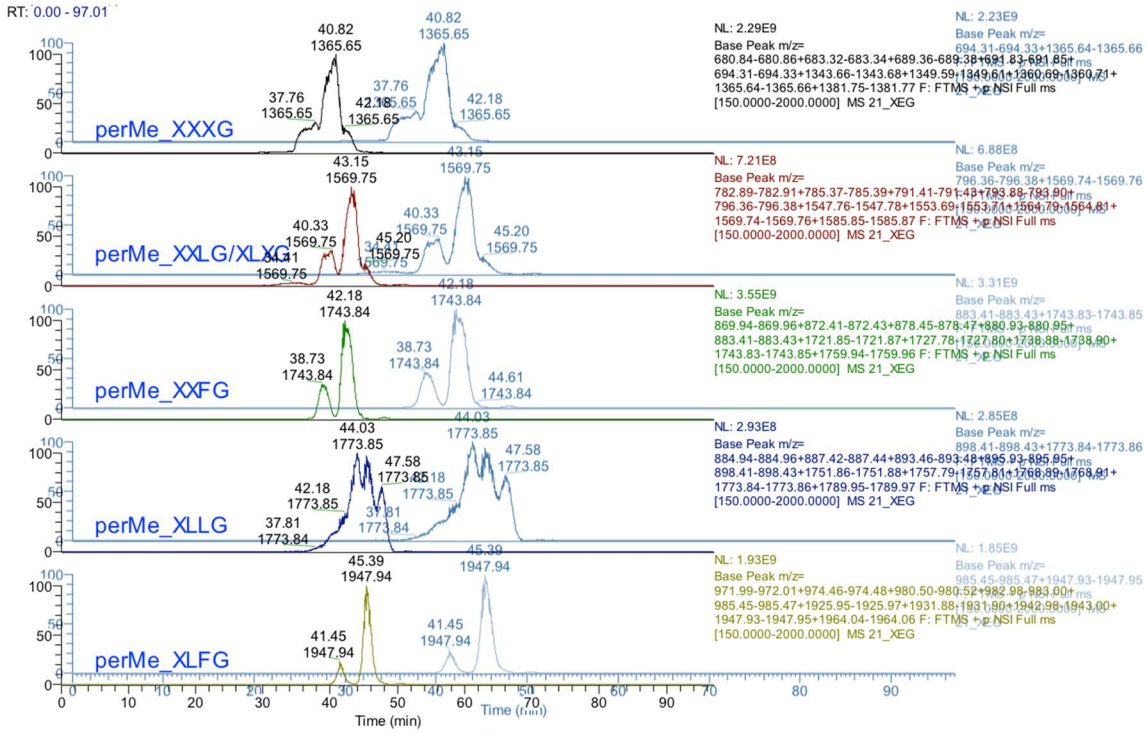

Figure 3.18 XG-pectin was digested with XEG, then analyzed on LC-MS. Left chromatogram set (dark colored) was permethylated xyloglucan subunits of all most possible ionized forms, right set (pale-blue) was sodiated xyloglucan subunits with permethylation. Peaks were labeled with apex retention time and base peak m/z.

Table 3.8 Calculated m/z used to screen chromatograms and peak areas

M	XXXG	XXLG/ XLXG	XXFG	XLLG	XLFG
$[M+H]^+$	1343.67	1547.77	1721.86	1751.87	1925.96
$[M+Li]^+$	1349.60	1553.70	1727.79	1757.80	1931.89
$[M+NH_4]^+$	1360.70	1564.80	1738.89	1768.90	1942.99
$[M+Na]^+$	**1365.65**	**1569.75**	**1743.84**	**1773.85**	**1947.94**
$[M+K]^+$	1381.76	1585.86	1759.95	1789.96	1964.05
$[M+H+NH_4]^{2+}$	680.85	782.90	869.95	884.95	972.00
$[M+H+Na]^{2+}$	683.33	785.38	872.42	887.43	974.47
$[M+2NH_4]^{2+}$	689.37	791.42	878.46	893.47	980.51
$[M+NH_4+Na]^{2+}$	691.84	793.89	880.94	895.94	982.99
$[M+2Na]^{2+}$	**694.32**	**796.37**	**883.42**	**898.42**	**985.46**
Peak area (all z=1 or 2)	5.00E+11	1.40E+11	5.30E+11	8.70E+10	1.90E+11
Peak area (only sodiated)	4.70E+11	1.30E+11	5.00E+11	8.30E+10	1.80E+11
Sodiated/All (area/area %)	92.40%	91.40%	94.90%	94.60%	94.70%

XG-Ara$_n$ was released from pectin network by enzymatically cleaving arabinan side chains of RG-I as above. There were still xyloglucan left in Peak 9 (figure 3.9, figure 3.10) that couldn't be released by arabinosidase and arabinanase, this portion of xyloglucan was presumed to be bound to pectin through the galactan side chains and/or arabinogalactan side chains of RG-I (Keegstra 1973). To investigate this possibility, endo-beta-(1,4)-galactanase (cloned from Emericella nidulans ORF AN5727) was used to hydrolyze aliquots of XG-pectin (Peak 3). Neutral products were purified with a PA1 cartridge, then digested with xyloglucanase, the XEG digest was permethylated, desalted and concentrated using a C18-ZipTip, then analyzed by LC-MS.

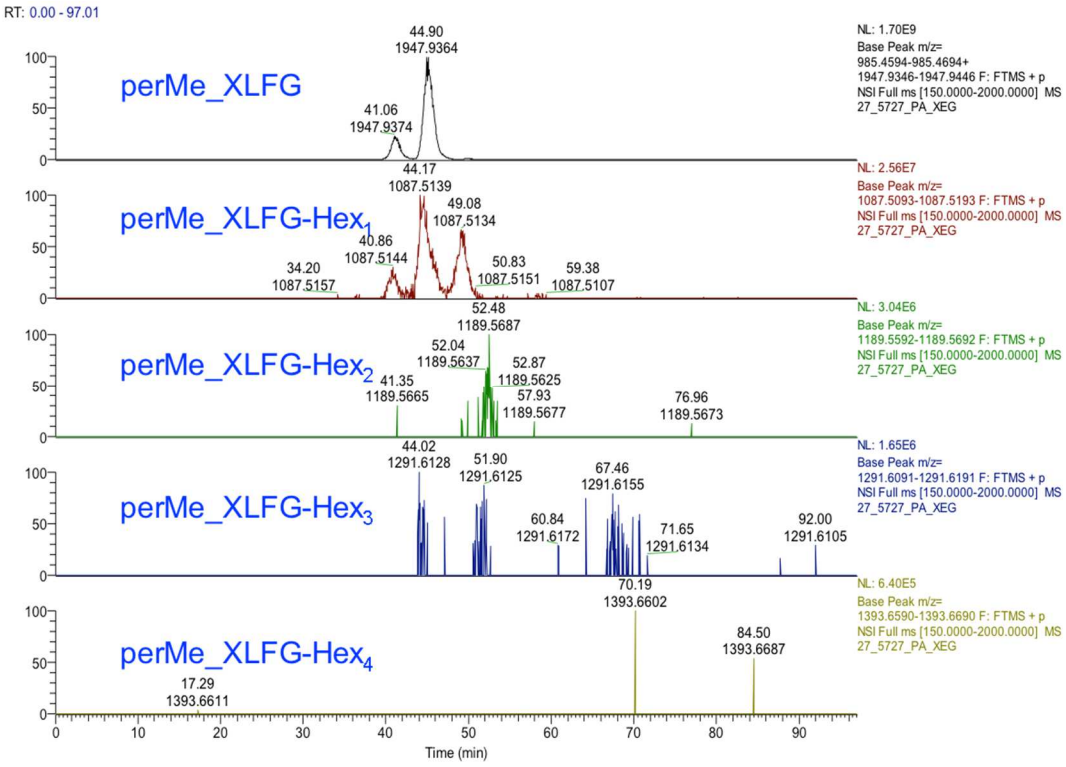

Figure 3.19 XG-pectin was digested with galactanase, neutral product was then digested with XEG, then analyzed on LC-MS. Chromatogram was set to display XLFG-Hex$_n$ (permethylated and sodiated). Peaks were labeled with apex retention time and base peak m/z.

Among the five predominant xyloglucan subunits in Arabidopsis, XXXG, XXLG, XLXG, XLLG are composed of only pentoses and hexoses, which share the same m/z values with isomers such as other hemicelluloses and/or arabinogalactans that may have been released by endo-galactanase. Thus only fucosylated subunits XXFG and XLFG were selected to detect the presence of an XG-pectin linkage, for instance XXFG-Ara_1 or XLFG-Ara_1 has a much lower chance to share the same m/z with isomeric contaminants. In the galactanase-xyloglucanase digestion product, only XLFG-Hex_n were screened to determine the presence of an XG-pectin linkage (figure 3.19), since XXFG-Gal_1 has the same m/z as XLFG. In figure 3.19, XLFG, XLFG-Hex_1 and XLFG-Hex_2 showed a basic trend of retention time shift as polarity of the mobile phase decreased. The MS/MS scan of XLFG-Hex_1 (m/z 1087.5156 at RT=44.11 min) was assigned, as glycosidic fragmentation in figure 3.20 was unique and adequate to prove the extra

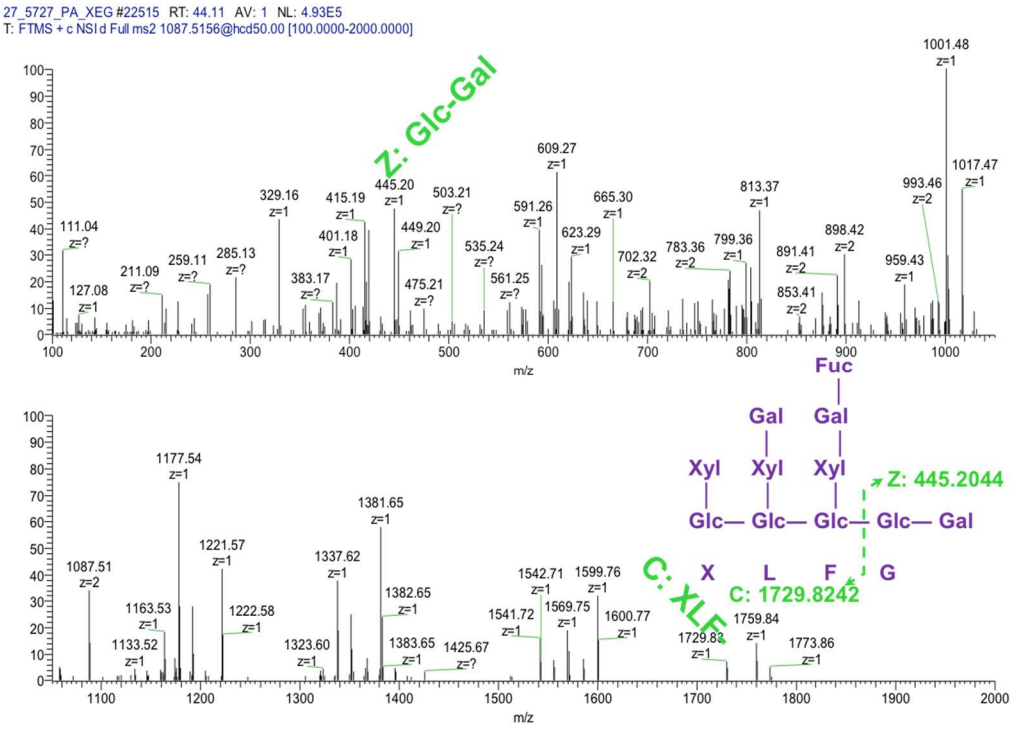

Figure 3.20 MS/MS spectrum of XLFG-Hex_1 in galactanase-xyloglucanase digestion. Peaks (permethylated and sodiated) were labeled with m/z and charge state.

hexose was at the reducing end of XLFG, and it was possibly galactose and responsible for the covalent bonding between xyloglucan and pectin. The peak area sum of XLFG-Hex_n (n=0,1,2…) was 1.6E+11, the peak area of XLFG-Hex_1 was 4.6E+9, without considering the impact that different XG side chains has on XG reducing end bond to pectin, only ~3% of galactanase-released XG subunits has putative hexose linkage, which makes it rather difficult to isolate adequate amounts for NMR analysis. Not only because of the little amount of XG_1-Hex_n, but also because the property of XG_1-Hex_n linkages are so close to XG subunits (XG_1), the peaks of those molecules are often overlapping in different HPLC methods, for example, similar retention times (RT) in figure 3.18, 3.19 and 3.21 indicate clustered elution.

Aliquots of XG-pectin (Peak 3) were digested with arabinosidase then arabinanase, neutral product were isolated with a PA1 cartridge and then hydrolyzed with xyloglucanase. The XEG digestion product was permethylated, desalted and concentrated with a C18-ZipTip, then analyzed by LC-MS (figure 3.21). We have already provided evidence that the extra pentose in XG_1-Pen_n, after a similar treatment procedure, is arabinose and that it is at the reducing end of xyloglucan. LC-MS, with high sensitivity and low detection limit, revealed more information. Processed LC-MS chromatograms showed XLFG-Ara_2 and XLFG-Ara_3, although peaks of XLFG with longer arabinose linkage were of low intensity, they showed a reasonable trend of peak shape at reasonable retention times. Moreover, although arabinanases cloned from hyperthermophilic bacteria tend to release oligo products from debranched arabinans: arabinose, arabinobiose and arabinotriose (F. M. Squina 2009, F. M. Squina 2010, Shi 2014); XLFG seemed to retain longer arabinan linkage than XXFG, possibly because more or longer side chains at reducing ends of xyloglucan chains hinder the access of the arabinanase to the arabinan linkage and leave longer tails. In the MS/MS spectrum of sodiated XXFG-Ara_1 (m/z = 963.4521, z=2,

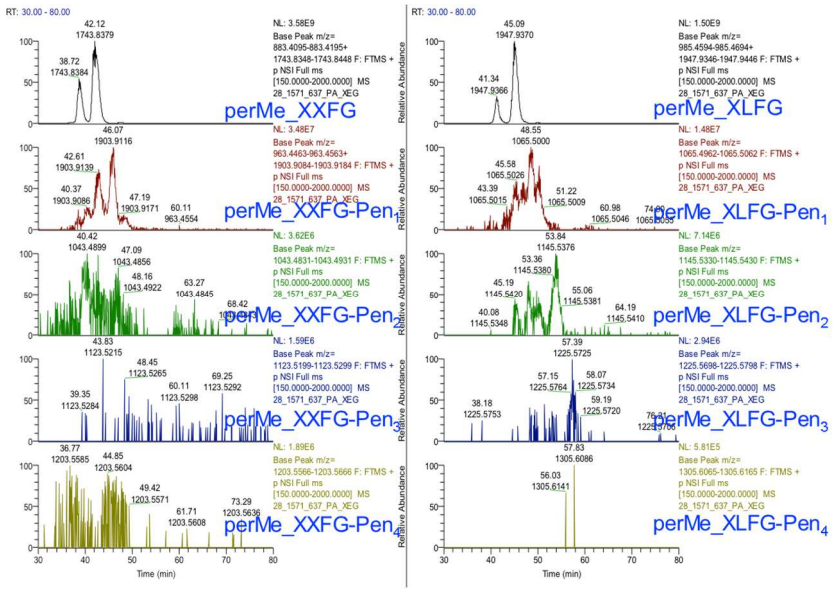

Figure 3.21 XG-pectin was digested with arabinosidase then arabinanase, neutral product was digested with XEG, and analyzed on LC-MS. Left chromatogram set was XXFG-Ara$_n$ (permethylated and sodiated), right chromatogram panel was XLFG-Ara$_n$ (permethylated and sodiated). Peaks were labeled with apex retention time and base peak m/z.

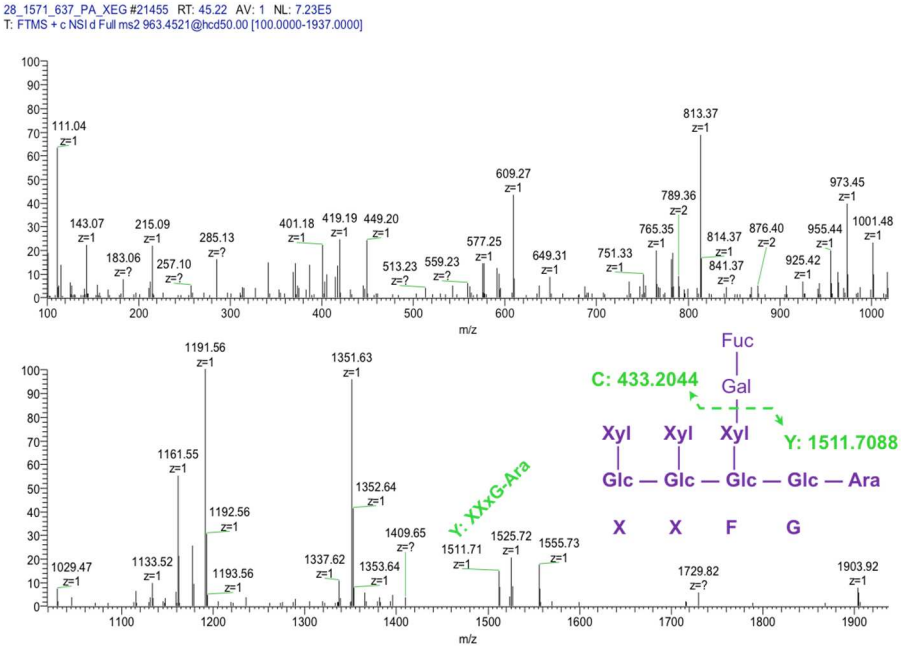

Figure 3.22 MS/MS spectrum of XXFG-Ara$_1$ in arabinosidase-arabinanase-xyloglucanase digestion. Peaks (permethylated and sodiated) were labeled with m/z and charge state.

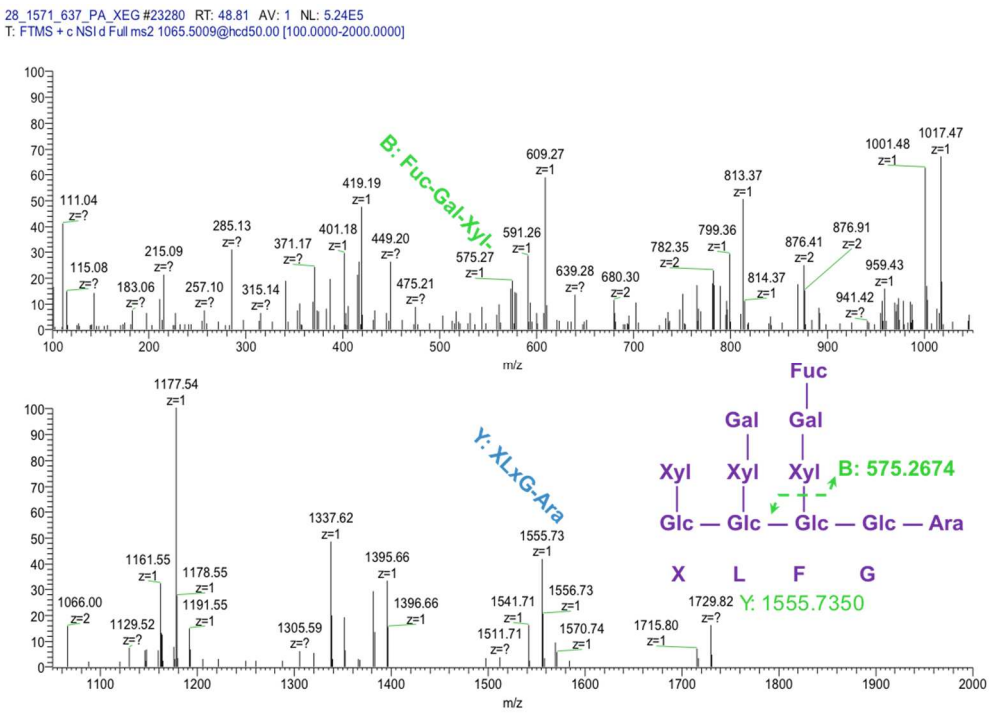

Figure 3.23 MS/MS spectrum of XLFG-Ara$_1$ in arabinosidase-arabinanase-xyloglucanase digestion. Peaks (permethylated and sodiated) were labeled with m/z and charge state.

at RT=45.22 min) (figure 3.22), fragmentation at the F side chain led to Y ions with a unique m/z of 1511.7088, similarly in the MS/MS spectrum of sodiated XLFG-Ara$_1$ (m/z 1065.5099, z=2, at RT=48.81 min) (figure 3.23), fragmentation at the F side chain led to B ions with a unique m/z of 575.2674, while other fragmented ions with different structure might share same m/z values. The peak area sum of X_FG-Ara$_n$ (n=0,1,2…; _ = X or L) was 6.0E+11, the peak area of X_FG-Ara$_n$ (n=1,2…; _ = X or L) was 1.2E+10, accordingly fucosylated linkage parts take ~2% among all fucosylated xyloglucan subunits, which indicates low linkage proportion within arabinanase-released xyloglucan.

3.2.3 Isolating XG-pectin linkage by trimming xyloglucan first

An aliquot of XG-pectin (Peak 3) was digested with xyloglucanase then arabinosidase, the negatively-charged product was purified with a PA1 cartridge. This should yield pectin with only short fragments of XG attached. This was then hydrolyzed with arabinanase to yield XG-arabinan fragments and high molecular weight pectin. Digestion mixture was separated with a VivaSpin concentrator (molecular weight cutoff, MWCO=10 kDa) and the low molecular weight product was permethylated, desalted, pre-cleaned and concentrated with a C18-ZipTip. It was then analyzed by LC-MS (figure 3.24). No XLFG-Ara_2 or XLFG-Ara_3 was detected in LC-MS chromatograms this time. Long-chain xyloglucan may adopt 'semi-flexible swollen coil' conformation (Muller 2011), which constitutes the stiffer domain of considerable size in the XG-pectin complex. If xyloglucan was chopped up first with xyloglucanase, the rest fragment were more flexible, the reducing end xyloglucan subunits left on arabinans might expose better as the arabinan side chains of RG-I swinging and bulging, which led to more thoroughly digestion by arabinosidase and arabinanase and XG_1-Ara_n linkage with even shorter oligo-arabinan.

In MS/MS spectrum of sodiated XXFG-Ara_1 (m/z 963.4507, z=2, at RT=44.78 min) (figure 3.25), fragmentation at backbone yielded Y ions with unique m/z of 1161.55, fragmentation at F side chain led to Y ions with a unique m/z of 1511.71 and m/z of 1715.81. Similarly in MS/MS spectrum of sodiated XLFG-Ara_1 (m/z 1065.5099, z=2, at RT=47.75 min) (figure 3.26), fragmentation at backbone led to Y ions with a unique m/z of 1161.55.

The peak area sum of X_FG-Ara_n (n=0,1,2…) was 2.0E+10, the peak area of X_FG-Ara_1 was 1.1E+9, accordingly fucosylated linkage parts take ~5% among all fucosylated xyloglucan subunits, which was estimated higher than cleave pectin first, if galactosylation in sidechain and arabinose residues at reducing end wouldn't affect the efficiencies of permethylation and ionization. In ideal circumstances, no matter xyloglucans were bond to pectin through arabinans

or galactans, trimming with xyloglucanase first was supposed to remove most of the xyloglucans including the tightly-entangled non-covalently linked xyloglucans from XG-pectin complexes, the xyloglucans left on pectin should be all bound to pectin covalently, however there were still a lot of xyloglucan without any linkage in the actual product that arabinanase stripped from pectin after xyloglucanase. Although covalently linked xyloglucan has been considered harder to get enzymatic access to than free xyloglucan, the network is still subtly intertwined shielding part of the xyloglucans from enzymes even with cellulose out of the picture. It was supposed to be easier to isolate the XG_1-Ara_n linkage from pectin side by size or by charge; however it turned out to be harder due to the complicated interaction between components.

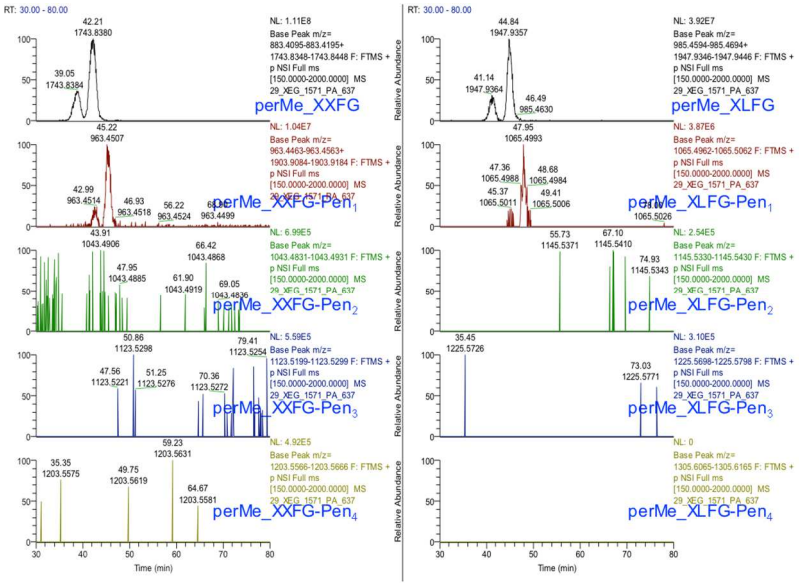

Figure 3.24 XG-pectin was digested with XEG then arabinosidase, charged product was digested with arabinanase, and analyzed on LC-MS. Left chromatogram set was XXFG-Ara_n (permethylated and sodiated), right chromatogram panel was XLFG-Ara_n (permethylated and sodiated). Peaks were labeled with apex retention time and base peak m/z.

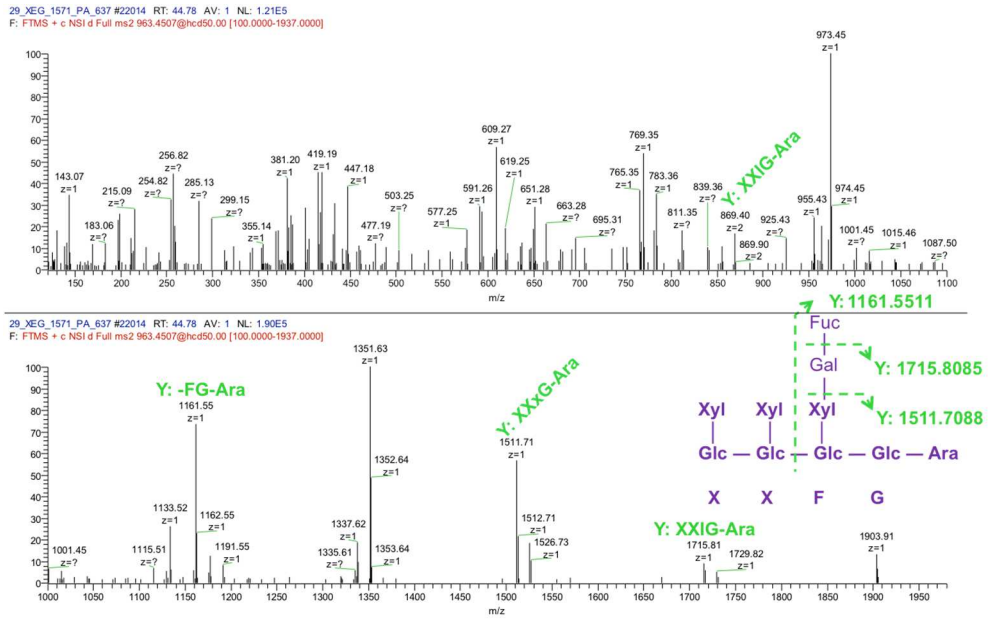

Figure 3.25 MS/MS spectrum of XXFG-Ara$_1$ in xyloglucanase-arabinosidase-arabinanase digestion. Peaks (permethylated and sodiated) were labeled with m/z and charge state.

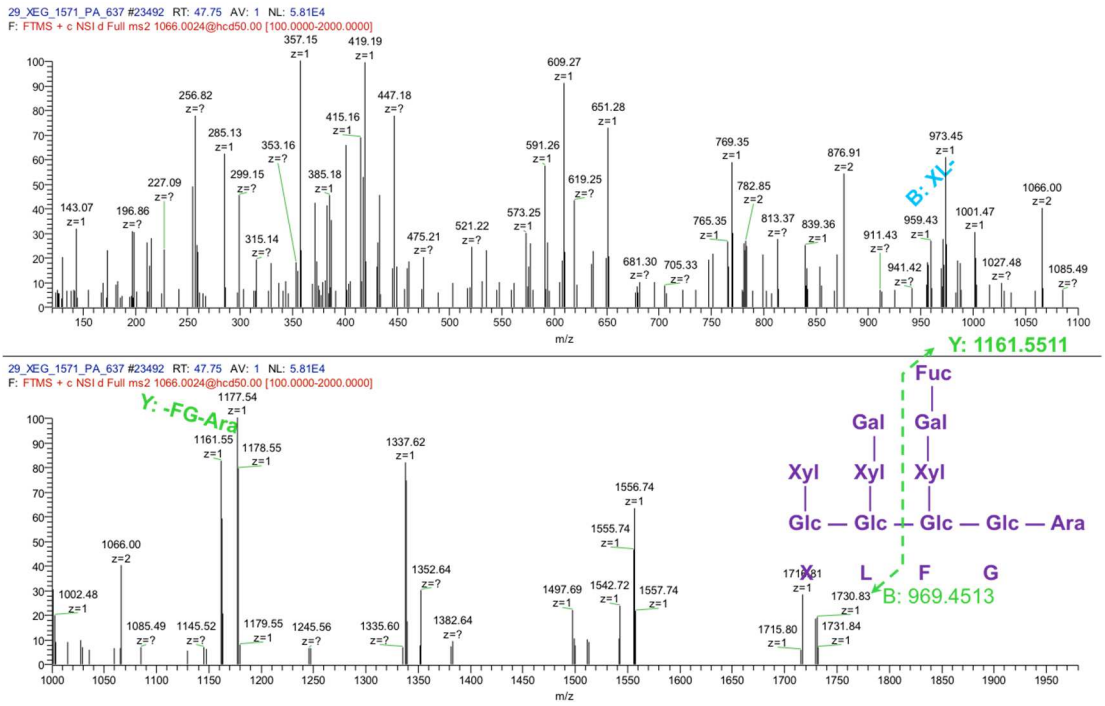

Figure 3.26 MS/MS spectrum of XLFG-Ara$_1$ in xyloglucanase-arabinosidase-arabinanase digestion. Peaks (permethylated and sodiated) were labeled with m/z and charge state.

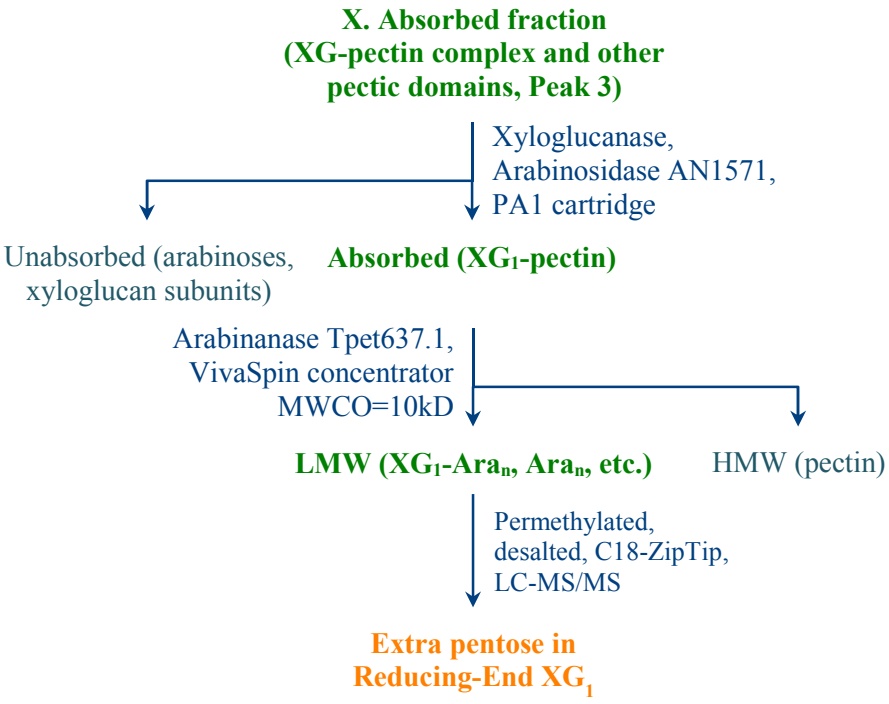

Figure 3.27 Experimental flowchart of isolating and analyzing XG-pectin linkage by trimming xyloglucan first.

3.3 XG-pectin linkage components found in other fractions of Arabidopsis cell walls

3.3.1 Detecting XG_1-Ara_1 in free xyloglucan

About half of the xyloglucans that solubilized from cell walls by strong alkali, was not bound to pectin, aliquot of these soluble electroneutral xyloglucans (Fraction IX, Peak 1 in figure 3.1) was hydrolyzed with xyloglucanase then permethylated, desalted and analyzed on LC-MS. Surprisingly, more XG_1-Ara_n were detected in this free xyloglucan fraction (figure 3.28). To further confirm the presence and position of the extra Ara_n, MS/MS spectra of relatively abundant X_FG-Ara_n were assigned (figure 3.29). The peak area sum of X_FG-Ara_n (n=0,1,2…) was 8.8E+11, peak area sum of X_FG-Ara_n (n=1,2…) was 5.9E+10, suggesting that ~7% of the free xyloglucan subunits has additional oligo-arabinan covalently bonded, if the structural and compositional differences between subunits didn't affect the efficiencies of permethylation and ionization when using standardized sample processing.

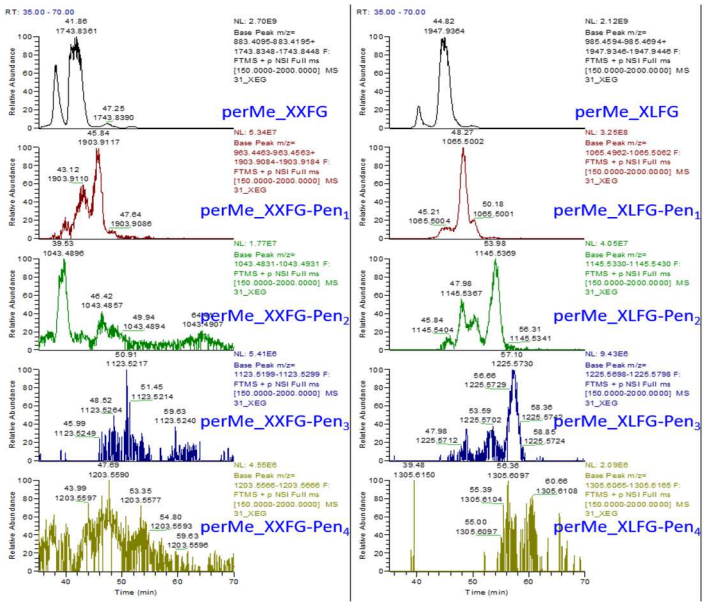

Figure 3.28 Neutral-soluble free XG was digested with XEG then analyzed on LC-MS. Left chromatogram set was XXFG-Ara_n (permethylated and sodiated), right chromatogram panel was XLFG-Ara_n (permethylated and sodiated).

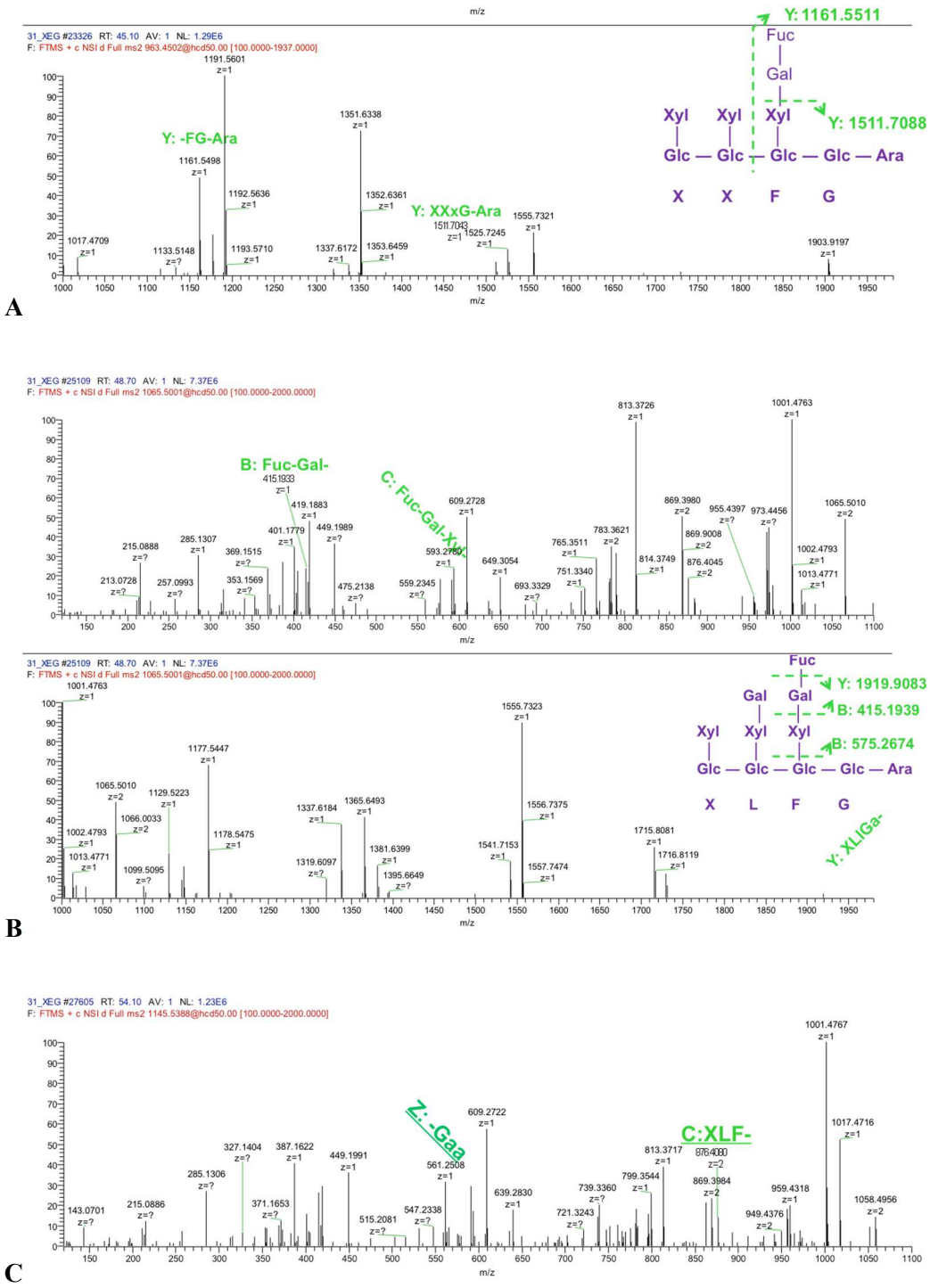

Figure 3.29 Neutral-soluble free XG was digested with XEG then analyzed on LC-MS^2. MS/MS spectrum of XXFG-Ara$_1$ (A), XLFG-Ara$_1$ (B), XLFG-Ara$_2$ (C), XLFG-Ara$_3$ (D).

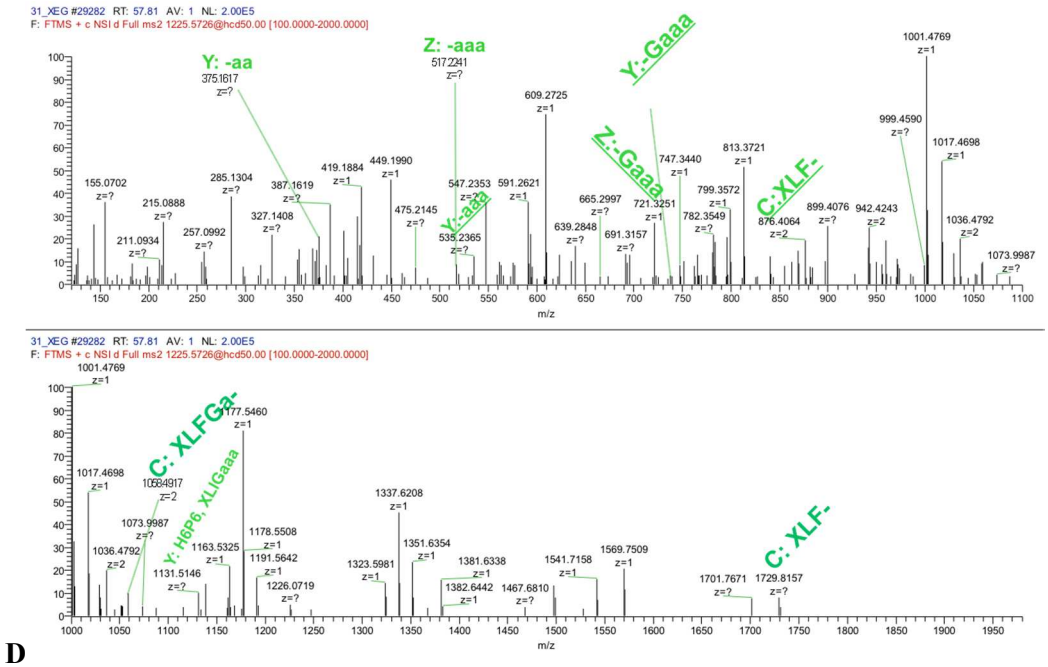

D

Figure 3.29 (Continued) Neutral-soluble free XG was digested with XEG then analyzed on LC-MS. MS/MS spectrum of XXFG-Ara$_1$ (A), XLFG-Ara$_1$ (B), XLFG-Ara$_2$ (C), XLFG-Ara$_3$ (D).

Free xyloglucan sample was analyzed on NMR spectroscopy. In HSQC (heteronuclear single quantum coherence, orange), carbon atom only correlates to the directly linked protons, whereas in HSQC-TOCSY (Total Correlation Spectroscopy) experiment (green), carbon atom correlates with all protons within the residue (figure 3.30). Superimposed HSQC-TOCSY and HSQC spectra excel at highlighting the whole residue peak pattern by relating cross peaks within same residue. Superimposed peaks were directly linked carbon and proton atoms, the other peaks in HSQC-TOCSY were carbons correlating with protons within the same residue but multiple bonds away, for instance, C1-H1 peak (superimposed) present in both spectra, the C1-H2 and C2-H1 peaks (green) in HSQC-TOCSY could help to navigate to C2-H2 cross peak (superimposed, related with dashed arrows).

Chemical shifts of atoms in furanose ring are usually greater than in pyranose ring. Signature peak patterns of arabinofuranose residues were distinguished from pyranoses (figure 3.30), the C5 of pentofuranose and C6 of hexose have similar chemical environment for CH_2OH groups, which leads to crowded and overlapping region. Inter-glycosidic cross peaks were assigned in HMBC, H4 of →5)-α-arabinofuranose-(1→ was noticed to correlate with C1 of unbranched Glc possibly through C5 of Ara (figure 3.31.B), and H1 of →5)-α-Ara*f*-(1→ correlated with C4 of reducing-end →5)-α-Ara*f* through 1,5-glycosidic bond (figure 3.31.A), which was consistent with the MS results that the reducing end Glc of xyloglucan was covalently linked to oligo-arabinan.

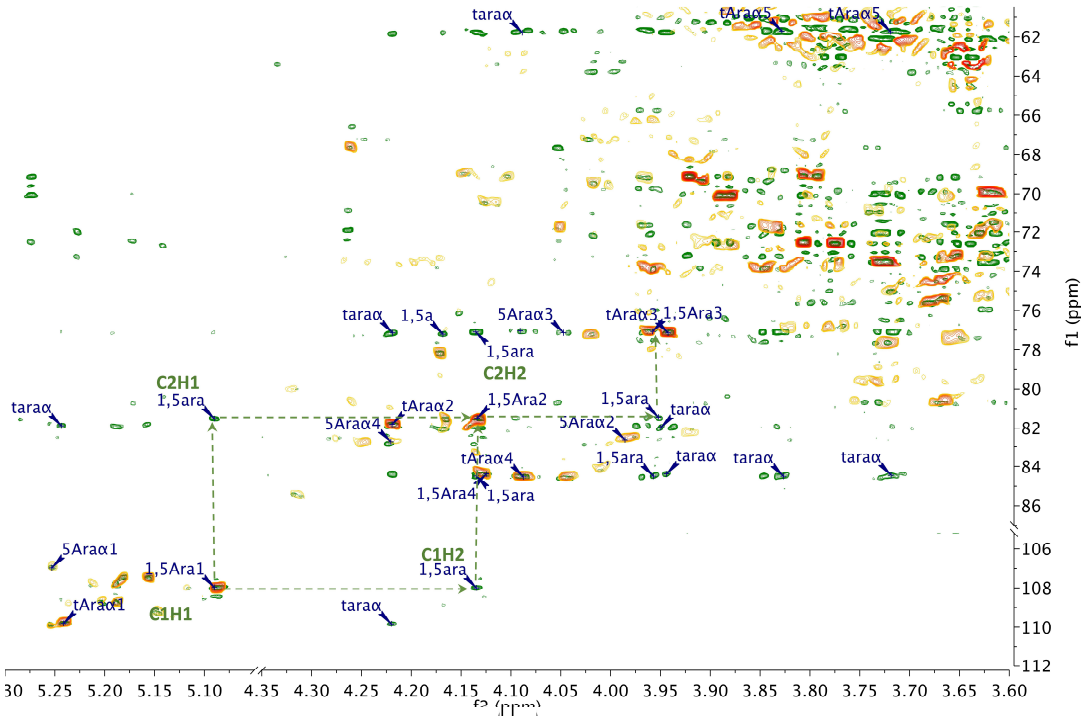

Figure 3.30 Selected regions of the superimposed HSQC-TOCSY and HSQC spectra of free XG (Peak1). HSQC-TOCSY spectrum (green) was laid above HSQC (orange) spectrum, superimposed peaks were directly linked carbon and proton atoms (capitalized). Only arabinose labels were shown due to limited space.

Table 3.9 NMR assignments of free XG (Peak 1).

Side Chain	Residue	C1	H1	C2	H2	C3	H3	C4	H4	C5	H5ax, H5eq	C6	H6, H6'
G.re	→4)-α-D-Glc*p*	92.62	5.23	72.04	3.54	71.91	3.83	80.82	3.53	71.85	4.05		
G.re	→4)-β-D-Glc*p*	96.45	4.64	74.70	3.24	76.43	3.48						
G.i	→4)-β-D-Glc*p*-(1→	102.94	4.55	73.34	3.40	75.37	3.66	80.69	3.73	75.65	3.68	61.78	3.94
X/L/F	→4,6)-β-D-Glc*p*-(1→	104.31	4.64	74.23	3.31	75.97	3.46	80.77	3.65			65.73	3.97
X	α-D-Xyl*p*-(1→	99.45	4.95	72.03	3.54	73.58	3.72	70.03	3.62	62.11	3.55, 3.72		
L/F	→2)-α-D-Xyl*p*-(1→	99.24	5.17	80.74	3.67	73.90	3.85	70.13	3.67	62.11	3.55, 3.71		
L	β-D-Gal*p*-(1→	105.03	4.55	71.51	3.62	73.17	3.65	69.15	3.92	74.46	3.67	61.63	3.77
F	→2)-β-D-Gal*p*-(1→	103.77	4.62	77.64	3.72	73.82	3.85					61.54	3.79
F	α-L-Fuc*p*-(1→	99.96	5.27	69.11	3.81	72.54	3.89	70.09	3.81	67.59	4.54	16.51	1.26
i	→5)-α-L-Ara*f*-(1→	107.98	5.09	81.48	4.13	77.06	3.96	84.38	4.12				
re	→5)-α-L-Ara*f*	106.97	5.25	82.62	3.99	77.13	4.05	82.72	4.22				
re	→5)-β-L-Ara*f*	92.62	5.23										
t	α-L-Ara*f*-(1→	109.81	5.24	81.81	4.22	77.14	3.94	84.53	4.09	61.71	3.83, 3.72		

Acetone in D_2O was chosen as internal reference: $\delta^{1}H$=2.22ppm, $\delta^{13}CH_3$=30.89ppm, $\delta^{13}CO$=215.94ppm (Nicholas R. Babij 2016). n.a.: not assigned. Re: reducing end, i: internal, t: non-reducing end terminal.

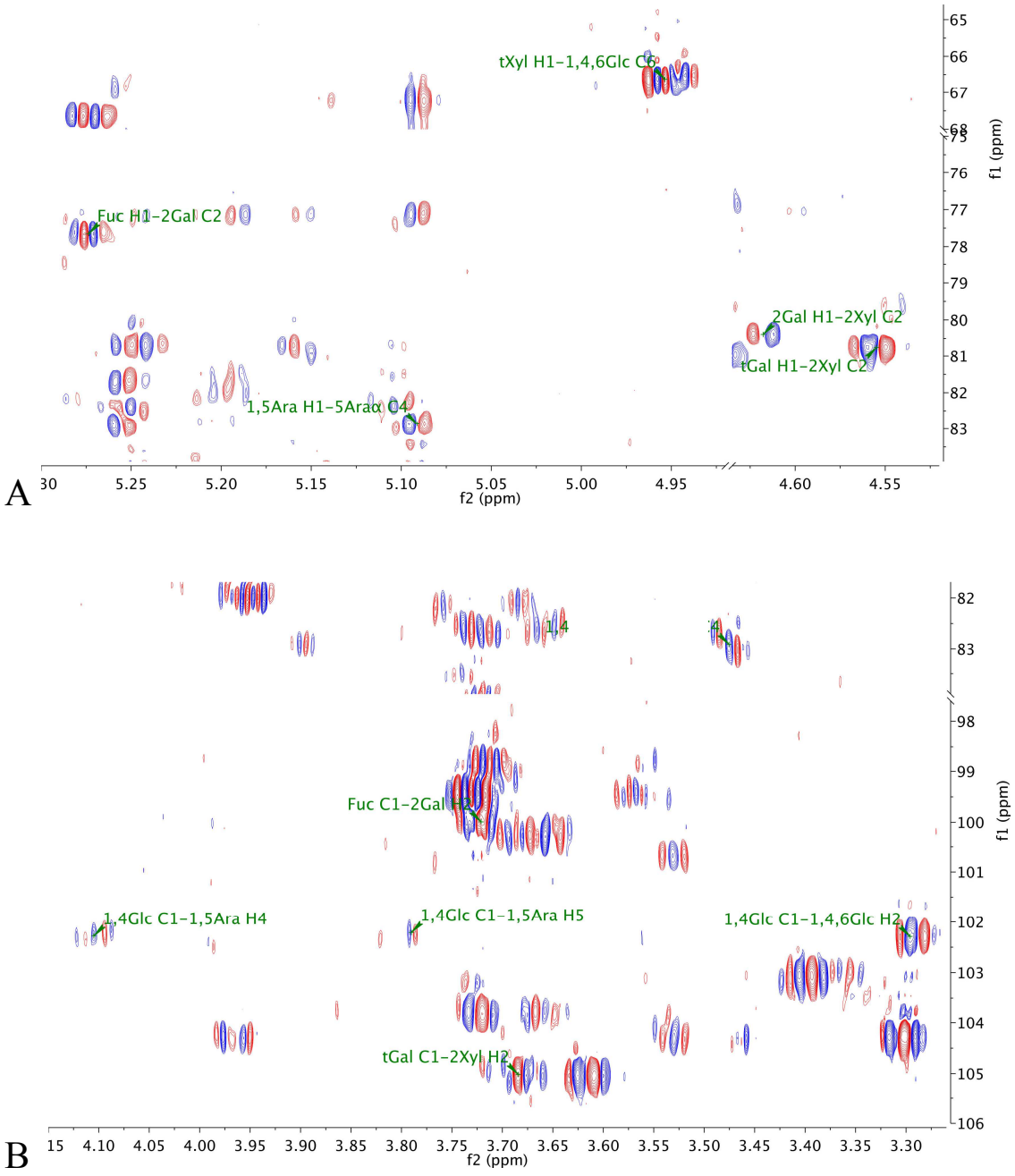

Figure 3.31 Selected regions of the heteronuclear multiple-bond correlation (HMBC) spectrum of free XG (Peak1). Only inter-glycosidic labels were shown due to limited space.

3.3.2 Detecting XG_1-Ara_1 in neutral-insoluble hemicelluloses

Xyloglucans was solubilized from cell walls by strong alkali, part of the xyloglucan precipitated after neutralization, can dissolve at pH>9. An aliquot of this neutral-insoluble portion (Fraction VIII, in figure 3.1) was hydrolyzed with xyloglucan then the supernatant of the digestion product was permethylated, desalted and analyzed on LC-MS. Again, XG_1-Ara_n were detected in this xyloglucan fraction (figure 3.32). MS/MS spectra were assigned (figure 3.33) to make sure the selected ions were X_FG-Ara_n. The peak area sum of X_FG-Ara_n (n=0,1,2…) was 4.4E+11, peak area sum of X_FG-Ara_n (n=1,2…) was 8.7E+9, there were ~2% of the neutral-insoluble xyloglucan has additional oligo-arabinan covalently bonded, if selected analytes had same permethylation and ionization efficiencies with standardized sample processing.

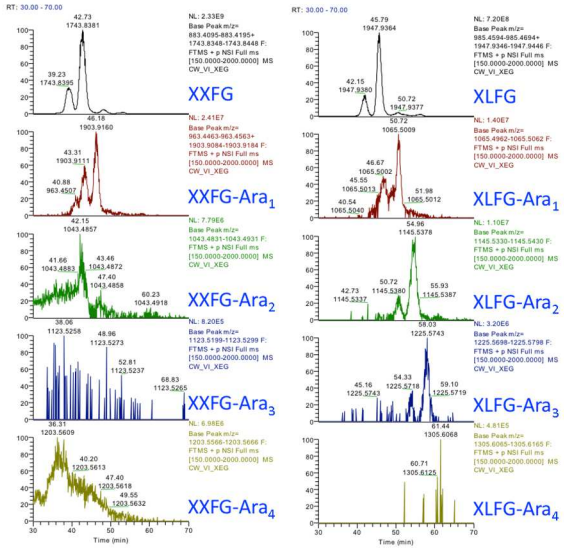

Figure 3.32 Neutral-insoluble XG was digested with XEG then analyzed on LC-MS. Left chromatogram set was XXFG-Ara_n (permethylated and sodiated), right chromatogram panel was XLFG-Ara_n (permethylated and sodiated).

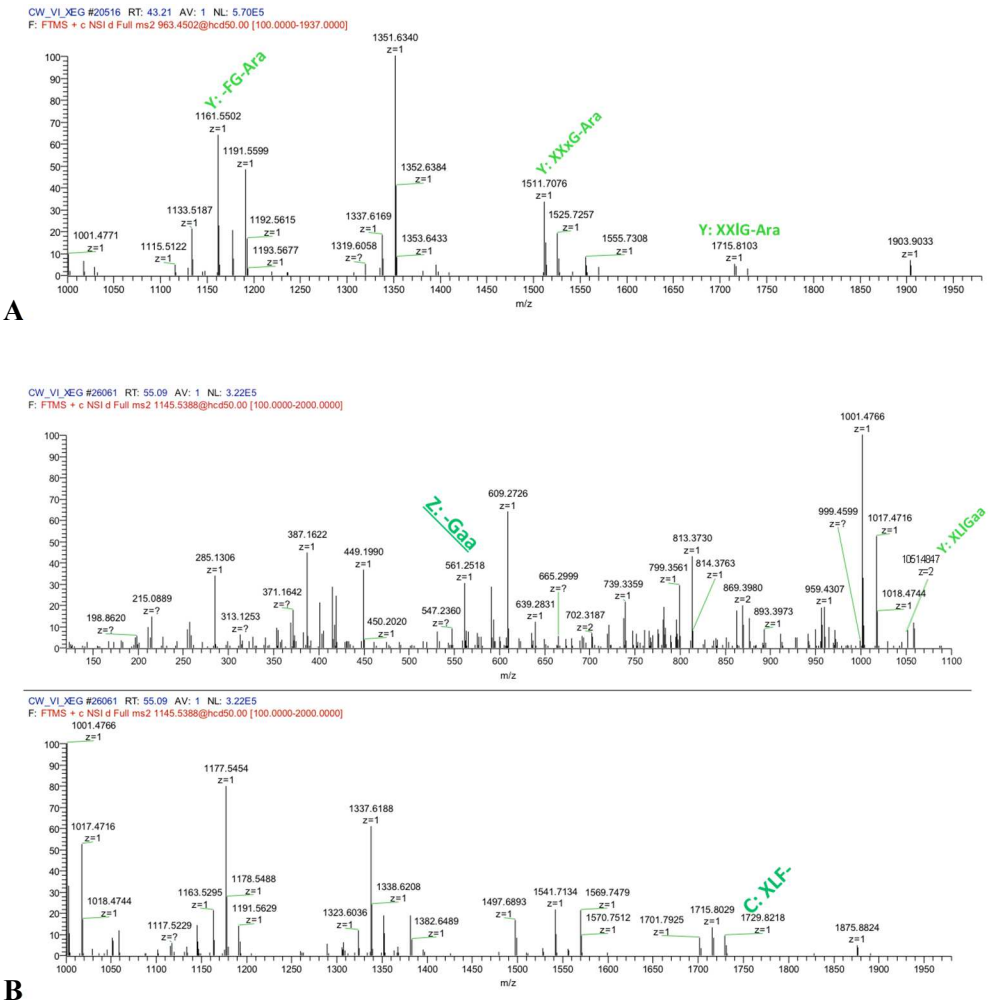

Figure 3.33 Neutral-insoluble XG was digested with XEG then analyzed on LC-MS^2. MS/MS spectrum of XXFG-Ara$_1$ (A), XLFG-Ara$_2$ (B).

No matter how XG-pectin was digested, from xyloglucan or from pectin first, there were always large amount xyloglucan without linkage left. While in the neutral-insoluble xyloglucan fraction and soluble electroneutral xyloglucan fraction, XG$_1$-Ara$_n$ were also detected. A possible assumption is, the integration between xyloglucan and pectin network is dynamically carried out during cellular growth and development, xyloglucans were not or not entirely bound to pectin de novo, XG-Ara$_n$ exist as relatively stable intermediates of crosslink synthesases or glycosyl-

transferases, when the structure of XG-pectin network needs to adapt to physiological functions, the linkage between xyloglucan and pectin could be broke with specific hydrolases, semi-ready XG-Ara_n of different lengths have different turnover rates in different cell wall proportions, i.e. neutral-insoluble hemicellulose component, unbound xyloglucan fraction and XG-pectin fraction.

3.4 Isolation and characterization of fluorescence-derivatized linkage between XG and pectin

Hydrolyzing xyloglucan first then isolating the XG-RG linkage from charged pectic network was not as efficient as expected, while cleaving pectin chains first left heterogeneous xyloglucan chains that were hard to separate. Thus, fluorescent molecules were added to the reducing ends of those detached xyloglucan chains by reductive amination (table 2.1), then after xyloglucanase digestion, purification was focused on reducing ends with fluorophores where the linkage was expected to be (figure 3.14). Charged fluorescence labels were first tried to differentiate reducing ends from the other XG subunits by charge state, however, APTS (8-aminopyrene-1,3,6-trisulfonic acid) was too difficult to elute when removing the excess labeling reagents. ANTS (8-aminonaphthalene-1,3,6-trisulfonic acid) labeled xyloglucan could be successfully cleansed and desalted with gel filtration but was too hard to elute from the PA1 column. Singly charged ANS (5-amino-1-naphthalenesulfonic acid, and 5-amino-2-naphthalenesulfonic acid) was easier to elute but insufficiently charged for large labeled molecules to bind to the anion exchange column (data not shown). Alternatively, an uncharged fluorophore 2-AB (2-aminobenzamide) was introduced to the neutral complexes for reducing-end tracing.

Xyloglucan-pectin complex (peak 3) was debranched with arabinosidase then cleaved with arabinanase to separate linkage from pectic polysaccharides using the PA1 column (figure 3.34, table 3.10). The unabsorbed neutral fraction (peak 31) was derivatized with 2-AB, then cleansed with an amino HILIC column (figure 3.35 A), monitored with tandem UV and evaporative light-scattering (ELSD) detectors. ELSD displays all analytes in the elution (green line), whereas UV only reveals fluorophore-attached molecules (red line). Tubing was minimized to reduce the void volume. Small molecules such as reducing salt and free 2-AB were eluted at low polarity (peak 34). The high molecular weight product (peak 35) was collected and

hydrolyzed with xyloglucanase, and then separated again on an amino column (figure 3.35 B). Most products revealed by MALDI-TOF MS were unsubstituted xyloglucan subunits (peak 37), singly galactosylated subunits (peak 38) and doubly galactosylated subunits (peak 39) (figure 3.36 A). Since there was only one reducing end in each xyloglucan chain, UV signal was magnified by five times when plotting for better comparative illustration (figure 3.35B).

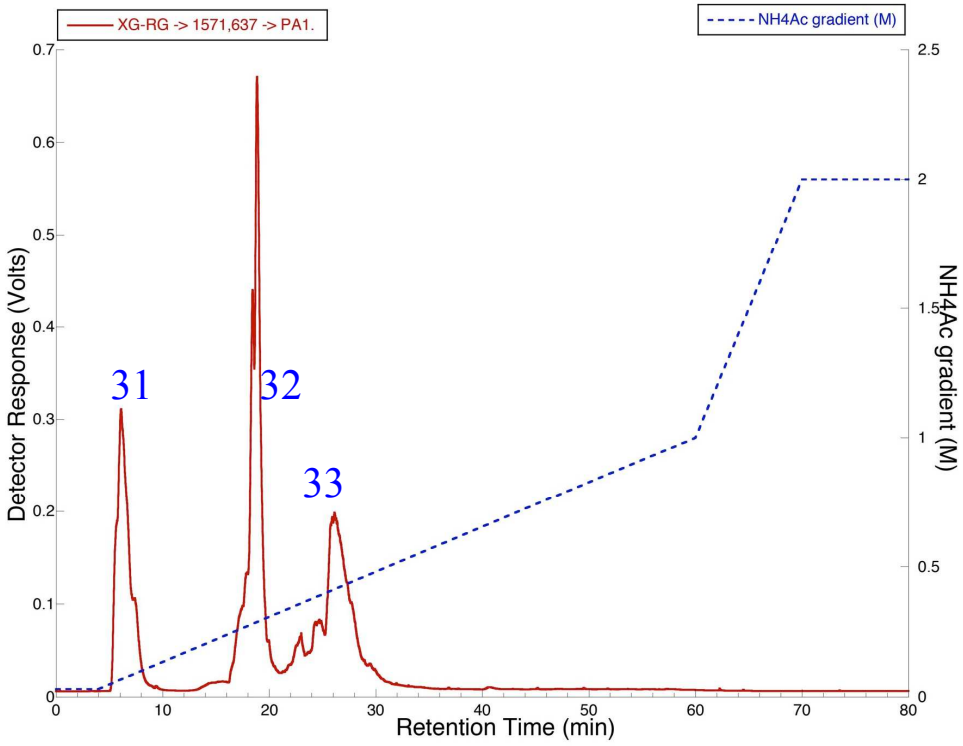

Figure 3.34 Arabinosidase (AN1571) and arabinanase (Tpet637) released neutral fraction was separated on PA1 column.

Table 3.10 Sugar compositions of PA1 separated arabinosidase and arabinase digestion

MOLE%	Ara	Rha	Fuc	Xyl	GalA	Gal	Glc
Peak31	9.7	n.d.	4.9	42.3	n.d.	12.9	30.2
Peak32	28.6	7.3	5.1	28.3	5.7	13.4	11.7
Peak33	8.1	24.5	1.2	7.5	39.0	16.5	3.1

* n.d.: not detected

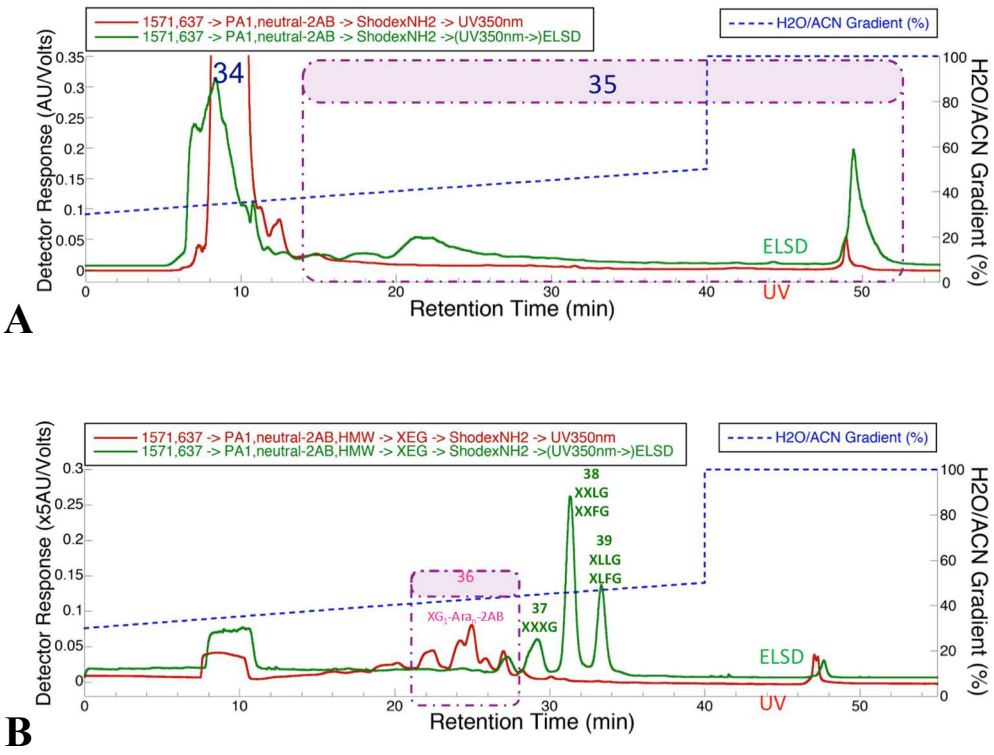

Figure 3.35 A. Neutral fragments released from XG-pectin complexes were derivatized with 2-AB and cleansed to remove excess labeling reagents on amino column. B. 2-AB-labeled neutral fragments were digested with xyloglucanase and separated on amino column again. HILIC elution was monitored with tandem UV detector (red) and ELSD (green).

AB derivatization successfully distinguished the reducing-end fragments from the rest of the xyloglucan repeating units but they may co-elute with underivatized smaller molecules (<1kD), also there might be reaction efficiency issues with the derivatization and permethylation, hence such methods could not compensate for the intrinsic low abundance of XG-pectin linkages. The fluorescent fractions contained mostly reducing ends of xyloglucan including the putative linkages, which apparently still contained a significant amount of xyloglucan units without arabinose (figure 3.36 B), the purification efficiency of XG_1-Ara_n was not ideal either.

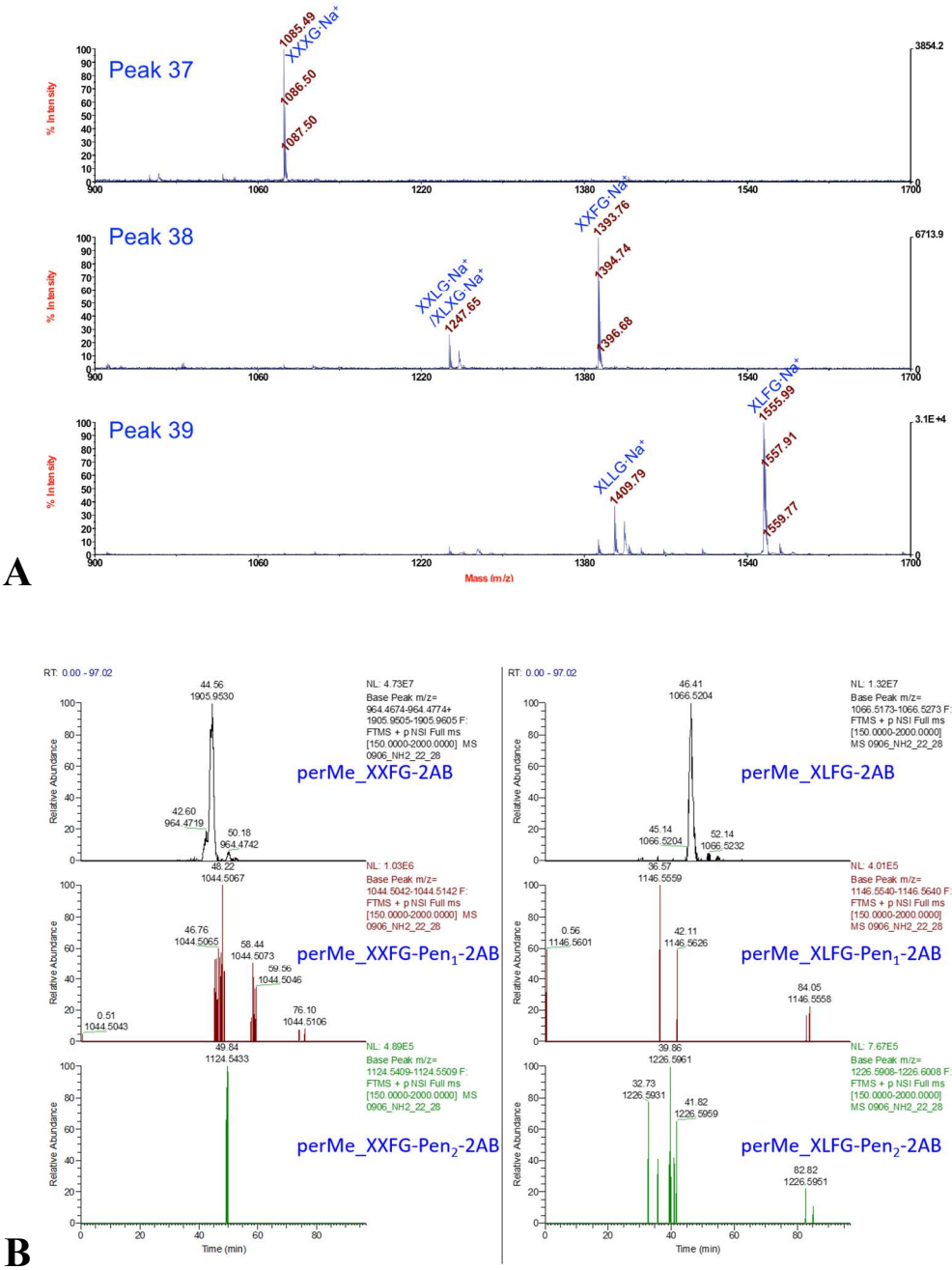

Figure 3.36 A. 2-AB-labeled neutral fragments were digested with xyloglucanase, fractions without fluorescence revealed by MALDI-TOF MS were native xyloglucan subunits as predicted. B. Fluorescent fractions (peak 36) were permethylated and analyzed with ESI-LC-MS, chromatogram of filtered m/z was shown.

To quantitatively and qualitatively estimate the reducing-end arabinose in xyloglucan, peak 36 was methanolysed with 1.5N HCl, then trimethylsilylated and analyzed on GC.

Commercial cellobiose (1,4-beta-D-glucobiose) and 1,5-alpha-L-arabinotetraose were derivatized with 2-AB as external standards, Glc_2, Glc_2-2AB, Ara_4, Ara_4-2AB were methanolysed, trimethylsilylated, and injected in the GC separately (figure 3.37). The sugar samples were broken into monosaccharides during methanolysis. Different reaction conditions affect the interconversion equilibrium between alpha and beta anomers and between pyranose and furanose cyclic forms (Mejanelle 2002), while trimethylsilylation reveils the difference between anomeric and cyclic conformations and presents four peaks (*αf, αp, βf, βp*) for each kind of monosaccharide. The sum of all four glucose peak areas reflects the amount of glucose in sample. Even though some peaks of different monosaccharides may have very similar retention times or may be too tiny to show up, bench-top GC still excels over MS for distinguishing isomeric residues, and over NMR for its thousand times lower detection sensitivity. NMR shows extreme overlap of signals from the ring protons. GC provides important complementary information of residue composition.

Reductive amination opens the cyclic ring of the reducing-end residue and consumes the C1 aldehyde group, thus 2-AB labeled monosaccharide only gives one peak compared with the corresponding native monosaccharide (figure 3.37). Comparing Ara_4 (orange) versus Ara_4-2AB (red), Glc_2 (lime) versus Glc_2-2AB (fern), the extra peak in 2-AB derivatized sample indicates the reducing-end residue with fluorescence attached, Ara-2AB or Glc-2AB (blue arrows). Glucofuranose peaks are both <1%, too small to notice; commercial arabinotetraose might contain some xylofuranose or other contaminants during industrial preparation as unexpected peaks shown in chromatogram (orange and red). In 2-AB labeled reducing-end subunits of xyloglucans which were released from XG-pectin complex (peak 36, cyan), as shown in LC-MS (figure 3.36), most xyloglucan reducing-end subunits had no arabinose attached and left backbone

glucose at reducing ends, thus Glc-2AB peak is present (cyan). However, the Glc-2AB peak was too small comparing with Glc peaks; and Ara-2AB peak was probably too small to notice comparing with significant Ara peaks. It seemed like the 2-AB derivatization yields were much lower than arabinotetraose and cellobiose. Same weight of samples was derivatized, for small molecules like Ara_4 and Glc_2, molar concentration of 2-AB was ~10 times of sample, for HMW sample like peak 31 (>10kD), the molar ratio between 2-AB and reactive reducing-end residues is >300. When excess fluorescent reagent and concentrated reducing salt are adopted in derivatization system, the reductive amination tends to complete reaction (Ruhaak 2010, Shilova 2003). Considering some small molecules (<1kD) without 2-AB might co-elute in Peak 36 after xyloglucanase digestion, it was unlikely including individual oligo-arabinans, which should have been eluted with excess 2-AB in Peak 34 (figure 3.38). The low efficiency of HMW sugar derivatization was probably due to the complex conformation of long xyloglucan chains which was described as 'semi-flexible swollen coil' (Muller 2011), and possible hindrance from fucosylated sidechains right next to reducing-end residues (only fucosylated subunits were specified in LC-MS spectra for less isomer). In addition, even for small molecules, derivatization of cellobiose seemed to have better yield than arabinotetraose, possibly also because curled conformation of 1,5- arabinan.

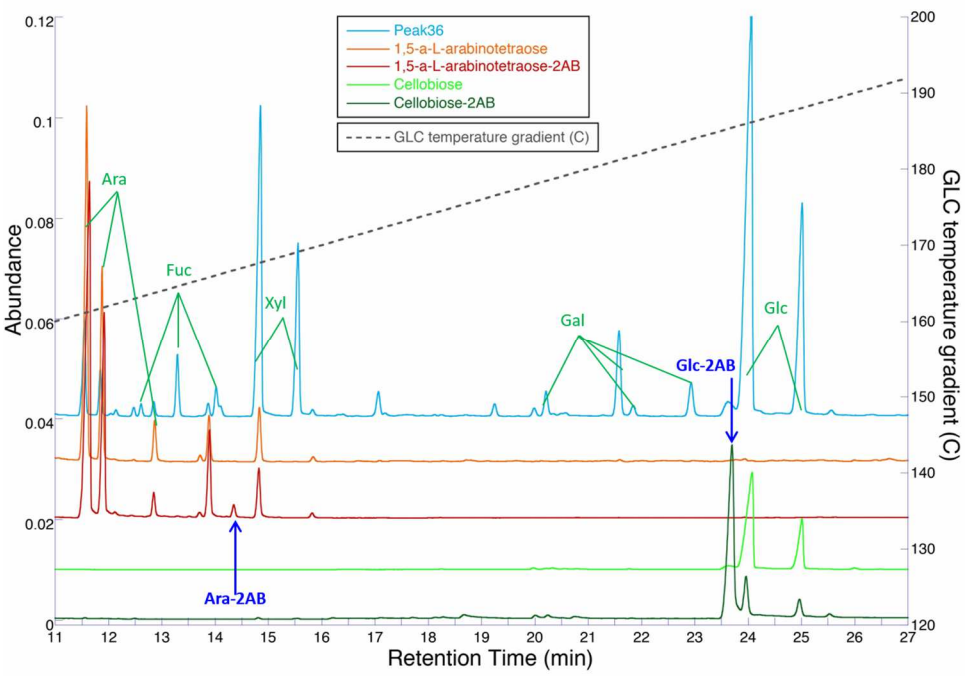

Figure 3.37 Gas chromatogram of 2-AB-labeled reducing ends of xyloglucans which were cleaved from XG-pectin complex (peak 36, cyan). Arabinotetraose (orange), arabinotetraose-2AB (red), cellobiose (lime), cellobiose-2AB (fern) were injected into GC separately as standards. All samples were methanolysed and trimethylsilylated for GC.

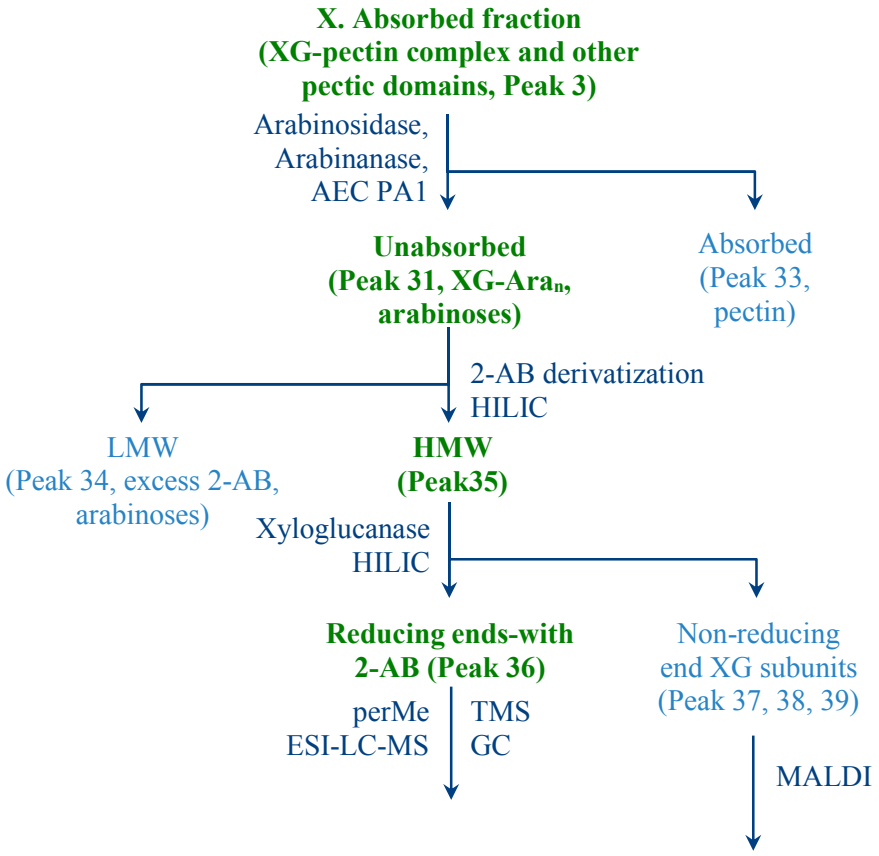

Figure 3.38 Experimental flowchart of isolating and analyzing fluorescence-derivatized XG-pectin linkage by trimming from pectin first.

3.5 Summary

Alkali-solubilized xyloglucan from arabidopsis culture cell walls was found either freely dispersed or bound tightly to pectic polysaccharides. Pectin-coeluted xyloglucan was dissociated from the acidic portions using various procedures combining enzymatic hydrolysis, HPLC, and derivatizing strategies.

Some of the native xyloglucan enzymatically released from pectin was found by CZE and MS to bear an additional pentose or pentoses at the reducing end of backbone. NMR analysis indicated the additional pentose in the endo-arabinanase released neutral product was an alpha-arabinofuranose. It is possible that the reducing end of xyloglucan links covalently to the arabinan sidechain of RG-I. A similar xyloglucan-oligoarabinan structure was also found in free xyloglucan as confirmed with LC-MS and NMR analyses. This xyloglucan-oligoarabinan might exist as an intermediate for XG-RG conjugation.

Xyloglucan was also released from pectin by endo-galactanase and found to have oligo-hexoses attached at the reducing end. Thus it is probable that XG can also be attached to RG through a pectic galactan linkage. This still needs to be further tested and verified. Derivatization at the reducing end of enzyme-released xyloglucan with fluorescent 2-aminobenzamide increased its hydrophobicity and facilitated its separation from native neutral sugars with similar size and composition. 2-Aminobenzamide derivatization may also differentiate the galactose residue at reducing end from galactose in XG sidechain using GC and/or MS, if derivatization efficiency could be further improved.

We noticed that some xyloglucan detached from the XG-RG complex when we debranched the pectic arabinan with exo-arabinosidase, or heated the complex at 80°C. Also, in the endo-arabinanase released neutral product, some xyloglucan had no additional pentose at the reducing end. These might be xyloglucans non-covalently bound to the pectin network. This non-

covalent interaction was so strong or extensive that it could survive or reform after strong alkali, heat, and concentrated salt elution. This explained the longer oligo-arabinan tail at the reducing end of xyloglucan when isolating XG-RG linkage by cleaving pectic arabinan first, because these non-covalently associated xyloglucans hindered the access of endo-arabinanase. The branched sidechains of RG-I played an important role in holding or shielding these non-covalent xyloglucans and might lead to the low yield of XG-RG linkage when trimming from xyloglucan first.

It is possible that, in the primary wall, the covalently linked xyloglucan is not or not entirely bonded to pectin de novo, xyloglucan-oligoarabinan exists as a relatively stable intermediate of conjugating enzymes such as xyloglucan endo-transglucosylase. When non-covalent XG-RG interaction is not adequate for structural integrity, semi-ready xyloglucan-oligoarabinan could immediately be linked with RG-I covalently to compensate. The XG-RG crosslink might be in a dynamic assembly and turnover, and the polymerization degree of each component could be adjusted during turnover for faster response using intermediates than synthesizing polymers de novo. This may help explain why significant changes of pectin or xyloglucan composition often do not affect the phenotype as expected (Kaewthai 2013, Cavalier 2008, Hocq 2020, Saez-Aguayo 2021, Hansen 2011), because diverse interactions between xyloglucan and pectin are combined, at various scales, at different locations, for different demands.

REFERENCES

ABRC. 2015. *Arabidopsis Biological Resource Center.* 11 24. Accessed 11 24, 2015. https://abrc.osu.edu/cell-culture.

Babij, N. R., McCusker, E. O., Whiteker, G. T., Canturk, B., Choy, N., Creemer, L. C., Amicis, C., Hewlett, N., Johnson, P., Knobelsdorf, J., Li, F., Lorsbach, B., Nugent, B., Ryan, S., Smith, M., Yang, Q. 2016. "NMR Chemical Shifts of Trace Impurities: Industrially Preferred Solvents Used in Process and Green Chemistry." *Organic Process Research & Development* 20: 661-667.

Bauer, S., Vasu, P., Persson, S., Mort, A. J., Somerville, C. R. 2006. "Development and application of a suite of polysaccharide-degrading enzymes for analyzing plant cell walls." *Proc Natl Acad Sci U S A* 103 (30): 11417-22.

Bauer, W. D., Talmadge, K. W., Keegstra, K., Albersheim, P. 1973. "The Structure of Plant Cell Walls: II. The Hemicellulose of the Walls of Suspension-cultured Sycamore Cells." *Plant Physiology* 51 (1): 174–187.

Bonnin, E., Le Goff, A., Körner, R., Vigouroux, J., Roepstorff, P., Thibault, J. F. 2002. "Hydrolysis of pectins with different degrees and patterns of methylation by the endopolygalacturonase of Fusarium moniliforme." *Biochim Biophys Acta* 1596 (1): 83-94.

Bythell, B. J., Abutokaikah, M. T., Wagoner, A. R., Guan, S., Rabus, J. M. 2017. "Cationized Carbohydrate Gas-Phase Fragmentation Chemistry." *J Am Soc Mass Spectrom* 28 (4): 688-703.

Carpita, N. C., Ralph, J., McCann, M. C. 2015. "The Cell Wall." In *BIOCHEMISTRY & MOLECULAR BIOLOGY OF PLANTS*, by Wilhelm Gruissem,and Russell L. Jones Bob B. Buchanan, 45-110.

Cassab, G. I. 1998. "Plant cell wall proteins." *Annu Rev Plant Physiol Plant Mol Biol* 49: 281-309

.

Cavalier, D.M., Lerouxel, O., Neumetzler, L., Yamauchi, K., Reinecke, A., Freshour, G., Zabotina, O. A., Hahn, M. G., Burgert, I., Pauly, M., Raikhel, N. V., Keegstra, K. 2008. "Disrupting two Arabidopsis thaliana xylosyltransferase results in plants deficient in xyloglucan, a major primary cell wall component." *Plant Cell* 20: 1519–1537.

Ciucanu, I., Kerek, F. 1984. "A simple and rapid method for the permethylation of carbohydrates." *Carbohydrate Research* 131 (2): 209-217.

Cui, M., Song, F., Liu, Z., Liu, S. 2001. "Metal ion adducts in the structural analysis of ginsenosides by electrospray ionization with multi□stage mass spectrometry." *Rapid communications in mass spectrometry* 15: 586-595.

Daas, P. J. H., Voragen, A. G. J., Schols, H. A. 2000. "Characterization of non-esterified galacturonic acid sequences in pectin with endopolygalacturonase." *Carbohydr Res* 326 (2): 120-9.

Darley, C. P., Forrester, A. M., McQueen-Mason, S. J. 2001. "The molecular basis of plant cell wall extension." *Plant Mol Biol* 47: 179-195.

Delaney, J., Vouros, P. 2001. "Liquid chromatography ion trap mass spectrometric analysis of oligosaccharides using permethylated derivatives." *Rapid Communications in Mass Spectrometry* 15: 325-334.

Fernández, L. E. M., Sørensen, H. R., Jørgensen, C., Pedersen, S., Meyer, A. S., Roepstorff, P. 2007. "Characterization of oligosaccharides from industrial fermentation residues by matrix-assisted laser desorption/ionization, electrospray mass spectrometry, and gas chromatography mass spectrometry." *Mol Biotechnol* 35 (2): 149-60.

Hansen, S. L., Ray, P. M., Karlsson, A. O., Jørgensen, B., Borkhardt, B., Petersen, B. L., Ulvskov, P. 2011. "Mechanical properties of plant cell walls probed by relaxation spectra." *Plant Physiol* 155 (1): 246-58.

Hocq, L., Guinand, S., Habrylo, O., Voxeur, A., Tabi, W., Safran, J., Fournet, F., Domon, J. M., Mollet, J. C., Pilard, S., Pau-Roblot, C., Lehner, A., Pelloux, J., Lefebvre, V. 2020. "The exogenous application of AtPGLR, an endo-polygalacturonase, triggers pollen tube burst and repair." *The Plant Journal* 103: 617-633.

Kaewthai, N., Gendre, D., Eklöf, J. M., Ibatullin, F. M., Ezcurra, I., Bhalerao, R. P., Brumer, H. 2013. "Group III-A XTH genes of Arabidopsis encode predominant xyloglucan endohydrolases that are dispensable for normal growth." *Plant Physiol* 161 (1): 440-54.

Keegstra, K., Talmadge, K. W., Bauer, W. D. and Albersheim, P. 1973. "The structure of plant cell walls: III. A model of the walls of suspension cultured sycamore cells based on the interconnections of the macromolecular components." *Plant Physiol* 51: 188–197.

Kiefer, L. L., York, W. S., Darvill, A. G., Albersheim, P. 1989. "Xyloglucan isolated from suspension-cultured sycamore cell walls is O-acetylated." *Phytochemistry* 28: 2105–2107.

Komalavilas, P., Mort, A. J. 1989. "The acetylation of O-3 of galacturonic acid in the rhamnose-rich portion of pectins." *Carbohydrate Research* 189: 261-272.

Laine, R. A. 1997. "Information capacity of the carbohydrate code." *Pure Appl. Chem* 69 (9): 1867-1874.

Ma, S., Lau, W., Keck, R. G., Briggs, J. B., Jones, A. J., Moorhouse, K., Nashabeh, W. 2005. "Capillary Electrophoresis of Carbohydrates Derivatized With Fluorophoric Compounds." In *Therapeutic Proteins. Methods in Molecular Biology*, by James D.C. (eds) Smales C.M., 397-409. Totowa, NJ: Humana Press.

McCann, M. C, Carpita, N. C. 2008. "Designing the deconstruction of plant cell walls." *Current Opinion in Plant Biology* 11 (3): 314-20.

Mejanelle, P., Bleton, J., Tchapla, A., and Goursoud, S. 2002. "Gas Chromatography-Mass Spectrometric Analysis of Monosaccharides after Methanolysis and Trimethylsilylation. Potential for the Characterization of Substances of Vegetal Origin: Application to the Study of Museum Objects." Chap. 24 in *Carbohydrate Analysis by Modern Chromatography and Electrophoresis*, by Ziad El Rassi, 845-902. Amsterdam: Elsevier Science.

Mort, A. J., BellEunice, G., Wu, X. 2013. "Characterization of a methyl-esterified tetragalacturonide fragment isolated from a commercial pectin with a medium degree of methyl-esterification." *Carbohydrate Research* 380: 108-111.

Mort, A. J., Wu, X. 2020. "Capillary Electrophoresis with Detection by Laser-Induced Fluorescence." In *The Plant Cell Wall. Methods in Molecular Biology, vol 2149*, by Zoë A. Popper, 45-56. New York, NY: Humana.

Muller, F., Manet, S., Jean, B., Chambat, G., Boue, F., Heux, L., Cousin, F. 2011. "SANS measurements of semiflexible xyloglucan polysaccharide chains in water reveal their self-avoiding statistics." *Biomacromolecules* 12: 3330–3336.

Oursel, S., Cholet, S., Junot, C., Fenaille, F. 2017. "Comparative analysis of native and permethylated human milk oligosaccharides by liquid chromatography coupled to high resolution mass spectrometry." *J Chromatogr B Analyt Technol Biomed Life Sci* 1071: 49-57.

Pabst, M., Kolarich, D., Pöltl, G., Dalik, T., Lubec, G., Hofinger, A., Altmann, F. 2009. "Comparison of fluorescent labels for oligosaccharides and introduction of a new postlabeling purification method." *Analytical Biochemistry* 384 (2): 263-273.

Park, Y. B., Cosgrove, D. J. 2015. "Xyloglucan and its Interactions with Other Components of the Growing Cell Wall." *Plant and Cell Physiology* 56 (2): 180–194.

Popper, Z. A., Fry, S. C. 2005. "Widespread occurrence of a covalent linkage between xyloglucan and acidic polysaccharides in suspension-cultured angiosperm cells." *Annals of Botany* 96 (1): 91-99.

Popper, Zoë A., Fry, S. C. 2008. "Xyloglucan-pectin linkages are formed intra-protoplasmically, contribute to wall-assembly, and remain stable in the cell wall." *Planta* 227 (4): 781-94.

Rabus, J. M., Abutokaikah, M. T., Ross, R. T., Bythell, B. J. 2017. "Sodium-cationized carbohydrate gas-phase fragmentation chemistry: influence of glycosidic linkage position." *Phys Chem Chem Phys* 19 (37): 25643-25652.

Ruhaak, L. R., Zauner, G., Huhn, C., Bruggink, C., Deelder, A. M., Wuhrer, M. 2010. "Glycan labeling strategies and their use in identification and quantification." *Anal Bioanal Chem* 397 (8): 3457–3481.

Saez-Aguayo, S., Parra-Rojas, J. P., Sepúlveda-Orellana, P., Celiz-Balboa, J., Arenas-Morales, V., Sallé, C., Salinas-Grenet, H., Largo-Gosens, A., North, H. M., Ralet, M. C., Orellana, A. 2021. "Transport of UDP-rhamnose by URGT2, URGT4, and URGT6 modulates rhamnogalacturonan-I length." *Plant Physiol* 185 (3): 914-933.

Serrat, M., Bermúdez, R. C., Villa, T. G. 2004. "Considerations on endopolygalacturonase activity and determination of comparison ratios with emphasis on the influence of the degree of substrate esterification." *J Agric Food Chem* 52 (6): 1534-1538.

Shi, H., Ding, H., Huang, Y., Wang, L., Zhang, Y., Li, X., Wang, F. 2014. "Expression and characterization of a GH43 endo-arabinanase from Thermotoga thermarum." *BMC Biotechnol.* 14 (35).

Shilova, N. V., Bovin, N. V. 2003. "Fluorescent labels for analysis of mono- and oligosaccharides." *Bioorg Khim* 29 (4): 339-55.

Squina, F. M., Prade, R. A., Wang, H., Murakami, M. T. 2009. "Expression, purification, crystallization and preliminary crystallographic analysis of an endo-1,5-a-L-arabinanase from hyperthermophilic Thermotoga petrophila." *Acta Crystallogr Sect F Struct Biol Cryst Commun.* 65 (pt9): 902–905.

Squina, F. M., Santos, C. R., Ribeiro, D. A., Cota, J., de Oliveira, R. R., Ruller, R., Mort, A. J., Murakami, M. T., Prade, R. A. 2010. "Substrate cleavage pattern, biophysical characterization and low-resolution structure of a novel hyperthermostable arabinanase from Thermotoga petrophila." *Biochem. Biophys. Res. Commun.* 399: 505-511.

Thompson, J. E., Fry, S. C. 2000. "Evidence for covalent linkage between xyloglucan and acidic pectins in suspension-cultured rose cells." *Planta* 211: 275-286.

Tran, N. T., Taverna, M., Deschamps, F. S., Morin, P., Ferrier, D. 1998. "Investigation of micelles and anionic cyclodextrins as pseudostationary phases for the capillary electrophoresis separation of oligosaccharides derivatized with 2-amino-benzamide." *Electrophoresis* 19 (15): 2630-8.

Vincken, J. P., Schols, H., Oomen, R., McCann, M., Ulvskov, P., Voragen, A., Visser, R. 2003. "If Homogalacturonan Were a Side Chain of Rhamnogalacturonan I. Implications for Cell Wall Architecture." *Plant Physiology* 132 (4): 1781–1789.

Wuhrer, M., Koeleman, C. A. M., Deelder, A. M. 2009. "Two-Dimensional HPLC Separation with Reverse-Phase-Nano-LC-MS/MS for the Characterization of Glycan Pools After Labeling with 2-Aminobenzamide." In *Glycomics: Methods and Protocols*, by Nicolle H. Packer and Niclas G. Karlsson, 79-91. Humana Press, a part of Springer Science + Business Media, LLC.

Zheng, Y., Mort, A. J. 2008. "Isolation and structural characterization of a novel oligosaccharide from the rhamnogalacturonan of Gossypium hirsutum L." *Carbohydrate Research* 343 (6): 1041-1049.

APPENDICES

NT-1 media for *Arabidopsis* T87 cell culture

800 ml ddH_2O, 4.3 g MS Salt, 30 g Sucrose, 0.18 g KH_2PO_4, 100 µl of 10 mg/ml Thiamine stock, 220 µl of 2 mg/ml 2,4-D stock, 100 mg *myo*-Inositol. Adjust the pH to pH 5.8 with 5M NaOH. Adjust the whole solution volume to 1 L. (ABRC 2015)

VITA

Xiaoyu Qiao

Candidate for the Degree of

Doctor of Philosophy

Thesis: CHARACTERIZATION OF THE LINKAGE BETWEEN XYLOGLUCAN AND PECTIN IN ARABIDOPSIS THALIANA CULTURE CELL WALLS

Major Field: Biochemistry and Molecular Biology

Biographical:

Education:

Completed the requirements for the Doctor of Philosophy in Biochemistry and Molecular Biology at Oklahoma State University, Stillwater, Oklahoma in June 2021.

Completed the requirements for the Master of Science in Biochemistry and Molecular Biology at the College of Life Sciences, Jilin University, Changchun, Jilin, China in 2012.

Completed the requirements for the Bachelor of Science in Biological Sciences at the College of Life Sciences, Jilin University, Changchun, Jilin, China in 2009.

Experience:

Graduate Research Assistant: Department of Biology and Molecular Biology, Oklahoma State University, Stillwater, Oklahoma, Aug 2013 to 2021.

Graduate Research Assistant: College of Life Sciences, Jilin University, Changchun, Jilin, China, Aug 2009 to Jun 2012.

Graduate Teaching Assistant: Experimental Cell Biology Course, College of Life Sciences, Jilin University, Changchun, Jilin, China, Spring 2010.